SYNTHESIS AND CHARACTERIZATION
OF
ORDERED MESOPOROUS SILICA FILMS
ON
OXIDIZED SILICON SUBSTRATES

A Thesis

Presented to the Faculty of the Graduate School

of Cornell University

in Partial Fulfillment of the Requirements for the Degree of

Master of Science

By

David Jacques Picciotto

January 2000

ABSTRACT

The fabrication of advanced electronic devices that operate on quantum effects requires the patterning of semiconductors on the scale of 50 Å, which cannot be achieved by any of the currently available patterning technologies. This project pursued a novel approach: the fabrication of a self-assembling template which would allow the deposition of ordered arrays of germanium dots on silicon substrates, on length scales permitting the operation of quantum devices at room temperature. The template is the mesoporous silicate MCM-41, discovered by researchers at Mobil Chemical Corp. This material consists of highly ordered, two-dimensional, hexagonal arrays of very uniform pores in silicon dioxide, with diameters tunable from 20 Å to over 100 Å.

If pore arrays of this material can be grown as thin films on silicon substrates, with the pores oriented normal to the substrate surface, the resulting structure will provide a template for the deposition of germanium dots. Germanium can then be deposited through the pores in the film and onto the silicon substrates by chemical or physical vapor deposition. The template film can then be etched away, leaving a hexagonally ordered array of germanium dots on the silicon substrate.

Mesoporous silica films were grown on oxidized silicon substrates by acidic synthesis. The substrates were first patterned by optical lithography to produce vertical features with dimensions of the order of microns. The substrates were then coated with hydrophobic polymer monolayers to alter their surface energy. This monolayer was selectively removed from the horizontal surfaces of some of the substrates, leaving it only on the vertical surfaces of the patterned features. It was thought that the difference in surface energy between horizontal and vertical

surfaces would induce the pores to align along the vertical surfaces. Additional engineering of these vertical surfaces, in the form of undulations, was expected to further confine the pores, such that their orientation would be normal to the horizontal substrate surface(s).

Samples consisting of mesoporous silica films on oxidized silicon substrates were characterized by transmission electron microscopy, scanning electron microscopy, atomic force microscopy, theta-two theta x-ray diffraction at both room and elevated temperatures, and x-ray diffraction pole figures.

The films, while displaying order, did not convincingly display hexagonal ordering, and possessed unwanted lamellar phases. The unwanted lamellar phases and minimal hexagonal ordering were probably due to a deficiency in the silica source in the synthesis reaction. The films were discontinuous, inhomogeneous, and very rough. No evidence was found to indicate that mesopores were preferentially ordered normal to the horizontal substrate surfaces. Neither was there any evidence found to indicate that mesopores were oriented with any preferential direction at all. However, x-ray diffraction results did suggest that controlling the surface energy of the substrate surface affected either the mesoporous silica films' structure, its orientation, or both.

TEM and x-ray diffraction were found to be the only reliable methods of characterization of samples at mesoscopic length scales. TEM specimen preparation of films was problematic and partially unsuccessful. Theta-two theta x-ray diffraction successfully yielded structural information for film samples. X-ray diffraction pole figures in reflection geometry were unsuccessful in determining mesopore orientation within films, because the available diffractometer could not be aligned with the precision necessary for the very small (~1.1°) incident angles required.

BIOGRAPHICAL SKETCH

David Jacques Picciotto was born August 16, 1959 in San Francisco, California and graduated from Monta Vista High School in Cupertino, California in June 1977. After briefly attending De Anza College in Cupertino, California, David spent fifteen years or so in materials management and production planning in the computer industry. In order to pursue a twenty-year old interest in physics, David entered North Carolina State University in May 1993, graduating summa cum laude in May 1997 with a Bachelor of Science degree in Physics. David entered Cornell University as a doctoral student in Applied Physics in June of 1997.

While pursuing research at Cornell, David became involved in science education outreach through the National Science Foundation-funded Cornell Center for Materials Research. Outreach work with children, experience designing lessons and curricula, taking an education course, and self-examination convinced David that a much greater contribution to society could be made through teaching than through research. Accordingly, he applied and was accepted into the Cornell Education Department's Master of Arts in Teaching Program, which he entered in August 1999.

David expects to teach high school physics, as well as some knowledge of the process of science, to a broad range of students. He hopes to contribute to the scientific literacy of all citizens.

This work is dedicated to my son, Daniel Jacques Picciotto, my wife, Alana Suzanne Jeydel, my parents, George Jacques and Camille Thompson Picciotto, the world's children in whom lies hope for the future, and to the Power that makes possible what is possible.

ACKNOWLEDGMENTS

The author wishes to thank and acknowledge the contributions of the following individuals, groups, and organizations:

Thanks to Professors E. Giannelis and C. Ober for their contributions, including the idea to use trenches and substrate surface energy modification to orient mesopores.

Thanks to Dr. G. Couillard for help with acclimation to the lab.

Thanks to Dr. S. Valiyaveettil, H. Chen, and M. Singh for introducing me to MCM-41 and sol-gel chemistry.

Thanks to N. Donnelly, C. Dunton, and D. Jacobs for assistance with mesoporous silica synthesis, calcination, and theta-two theta x-ray diffraction.

Thanks to T. Dalrymple and N. Nemchuk for substrate processing.

Thanks to Y. Takamura for her very good initial work on fluoropolymer coating and ion milling.

Thanks to N. Donnelly for the initial work on x-ray diffraction pole figures, and for further developing Y. Takamura's work with fluoropolymer-coated substrates and anisotropic coating removal by ion milling.

Thanks to W. Qin for teaching me to use the enlarger and print processor.

Thanks to Dr. T. Kamins of Hewlett Packard Laboratories in Palo Alto, California for performing the AFM studies included in this work.

SEM micrographs were obtained by G. Nagy of the Cornell Nanofabrication Facility, and by C. Dunton, a student in the Department of Material Science and Engineering at Cornell. Thanks to both.

Characterization by TEM, optical microscopy, and x-ray diffraction was performed in facilities of the Cornell Center for Materials Research (CCMR),

funded by the National Science Foundation under grant number DMR-9632275. TEM work, sample preparation, and most of the darkroom work was performed by Dr. N. Jiang of CCMR. Thanks to J. Hunt of CCMR for training in microscopy. Special thanks to Dr. M. Weathers of CCMR, for assistance with x-ray pole figures, high-temperature diffraction experiments, and long hours of discussion.

This work was performed in part at the Cornell Nanofabrication Facility (a member of the National Nanofabrication Users Network) which is supported by the National Science Foundation under Grant ECS-9319005, Cornell University, and industrial affiliates.

Thanks to Professor J. Brock for perspective and for serving as chair of my Special Committee.

A very special thanks to Dr. K. Edler, late of the Cornell University Physics Department and now at the University of Bath, for countless hours of discussion on the formation, synthesis, and characterization of MCM-41.

Special thanks to my adviser, Professor D. Ast for all of his support and suggestions, including, but certainly not limited to, the idea to use x-ray diffraction pole figures to determine mesopore orientation.

Special thanks to Eastman Kodak Company for the very generous Kodak Fellowship that supported my studies and research, and thanks to Dr. G. Bottger, Ms. E. Brooks, and Mr. P. Fleming of Kodak for taking such an interest in my work.

The funding for this research was provided by the Defense Advanced Research Projects Agency (DARPA) under grant number N66001-97-1-8922.

TABLE OF CONTENTS

LIST OF TABLES

LIST OF FIGURES

CHAPTER ONE: INTRODUCTION

As conventional microelectronic devices and integrated circuits shrink in size toward their ultimate limits, researchers have turned their attention to the question of what happens next. One of the wilder-sounding schemes is quantum computing. The fundamental unit in quantum computing and data storage is the qubit, short for "quantum bit". In a conventional digital computer, bits may take on one of two values, 0 or 1. A qubit is also a two-state system, but it is a quantum system. Therefore, superpositions of the two states are possible. The basic principle in quantum computing is that information can be stored and manipulated in these qubits as superpositions of the allowed states in the physical realization of the qubit. If the physical realization is hydrogen nuclei in some small organic molecule, the states are nuclear spin states. In a quantum dot, the states are electronic energy levels. A physical realization of a quantum computer will consist of a collection of qubits (i.e. a quantum system made up of 2-state quantum subsystems) that are acted upon by some Hamiltonian that constitutes the program.

Initial work in quantum computing was theoretical, beginning with Feynman[1,2] in 1982. A number of theoretical advances over the years were followed by Shor's 1994 breakthrough development of a quantum computing algorithm for factoring large integers[3]. On a digital computer, the number of steps required for this task is exponential in the input size (number of digits in the integer). Consequently, an assumed inability to factor large numbers into primes is a common basis for cryptographic schemes. However, Shor's algorithm for a quantum computer requires a number of steps that is only polynomial in the input size. A second breakthrough came in 1997 with Grover's discovery of a quantum algorithm for doing fast searches of a database[4]. An exhaustive search of an N-item

database by a digital computer for an item meeting certain criteria, requires N steps to find the item with certainty. Grover's algorithm for a quantum computer requires only $N^{1/2}$ steps. In both of these cases, the speed arises from the fact that the quantum computer is able to perform computations on superpositions of states. It can thus operate on multiple pieces of information simultaneously.

Experimental advances have been very slow in coming. For several reasons, it has proven to be difficult to actually build a quantum computer. The first demonstration of a quantum logic gate was made by Monroe, et al.[5] in 1995. The system was a trapped atom laser cooled to zero-point energy, and stored two qubits. One qubit consisted of two hyperfine states and the other consisted of two quantized harmonic oscillator states. Experimental demonstrations of systems actually running quantum algorithms were reported for the first time in 1998. Two groups[6,7] implemented Grover's fast search algorithm in nuclear magnetic resonance (NMR) systems using organic molecules. In these realizations, nuclear spin states form the qubits, and the systems had four states.

One of many problems in the development of quantum computers is scaling the system up to large numbers of qubits so that nontrivial computations can be made. Solid state systems may have advantages over NMR and trapped ion systems in this regard. The first experimental demonstration of control of a solid state qubit was made by Nakamura, et al.[8] in April 1999. No logic gate or running algorithm has yet been demonstrated on a solid state system.

Quantum computing is of interest for at least two practical reasons, in addition to theoretical interest and novelty/curiosity value. The first practical reason is speed. The two types of problems for which it is known that quantum computers can significantly outperform digital computers have been mentioned above. The

second practical reason is that, in principle, very small sizes for the computer can be achieved, especially in solid state realizations.

In a solid state realization of a quantum computer, one would like to have large numbers of identical quantum dots. One would like the machine to operate at room temperature, avoiding the need for cryogenics. In order to have reliable room temperature operation, the dots must be small enough such that their electronic energy level spacing is comfortably greater than k_BT, the thermal energy of electrons at room temperature. To a first approximation, the electronic energy levels in the dots are simply the energy levels of non-interacting particles in a square well potential. Therefore, the energy level spacing is inversely proportional to the size of the dot, and a quick calculation shows that one would like dots no bigger than 50 Å for energy spacings greater than k_BT.

Patterning on length scales of 50 Å and less is beyond the reach of conventional technology, including e-beam and x-ray lithography. Even if patterns could be written this small, the time it would take to write them for ~10^{12} devices per square centimeter would be prohibitively long. Consequently, the problem lends itself to a solution involving self-assembly.

The present work is concerned with employing a self-assembling technique to produce a template to pattern 2-dimensional hexagonal arrays of germanium quantum dots on oxidized silicon substrates. The template has dimensions consistent with the operation of quantum devices at room temperature, that is, 50 Å or less. The template is the mesoporous silicate MCM-41[9], discovered by researchers at Mobil Chemical [10,11], and is formed from the liquid phase. This material consists of highly ordered, two-dimensional, hexagonal arrays of very uniform pores in silicon dioxide, with diameters tunable from 20 Å to over 100 Å. Pore arrays of this material were grown as films on oxidized silicon substrates. The

objective was to have the pores oriented normal to the substrate, to provide the template for the germanium dots. Germanium could then be deposited through the pores in the film and onto the silicon substrates by chemical or physical vapor deposition. The film could then be etched away, leaving a hexagonally ordered array of germanium dots on the silicon substrate.

CHAPTER TWO: BASIC PRINCIPLES

Formation of Mesoporous Silicates

The use of organic materials as templates to produce ordered porous inorganic materials has resulted in the discovery and development of a vast array of new materials. One subset of these materials is mesoporous silicates[10-16], which possess pores ranging in diameter from about 20 Å to over 100 Å. Various organics have been used to template these silicates, including a wide range of surfactants[10-26] and block copolymers[27,28]. The present work focuses on templating mesoporous silicates using cationic surfactants.

Using surfactant templates, mesoporous silicates are formed in (usually aqueous) solution. All that is needed is water, surfactant, a silicate source, and acid or base conditions to catalyze the polymerization of the silicate. The surfactant molecules utilized in the present work have hydrophilic heads and hydrophobic carbon tails. In sufficient concentrations in aqueous solution, these surfactant molecules will spontaneously self-organize into cylindrical micelles in order to minimize the interface between the hydrophobic portion of the surfactant molecules and the aqueous phase (see Figure 2.1). These micelles have a bottle brush appearance, with the individual molecules forming the "bristles" of the "brush", and the hydrophobic tails at the center of the micelle, away from the aqueous phase. The length of the surfactant molecule, which is a function of the number of carbon atoms in the chain, determines the micelle diameter.

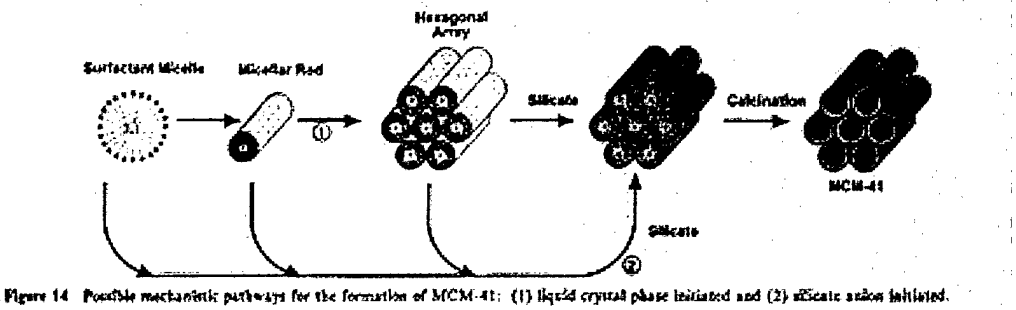

Figure 2.1: MCM-41 formation process as proposed by Beck, et al.[11] Figure taken from reference 11.

The cylindrical micelles will themselves self-assemble into regular arrays. The structure of these arrays (lamellar, cubic, or 2-dimensional (2-D) hexagonal) is determined by both the surfactant and silicate concentrations. In the present work, it is the 2-D hexagonal phase that is of interest. Once the micelles have self-assembled, the silicate polymerizes around them, until after a time that depends on temperature and other factors, there is a continuous phase of what is generally presumed to be amorphous silicon dioxide surrounding all the micelles.

The exact process by which mesoporous silicates are formed is not completely understood. One model, proposed by Beck, et al.[10,11], invokes a liquid crystal templating mechanism. In this model, the surfactant micelles self-organize into various liquid crystal phases that depend on surfactant concentration in the reaction vessel, after which silica infiltrates the spaces between the micelles and polymerizes (see Figure 2.1). In a second model, proposed by Davis, et al.[29], a layer of silica surrounds individual micelles which then organize into a hexagonal (or other) phase, following which the silica polymerizes (see Figure 2.2). Davis, et al.[29]

present strong evidence obtained by ^{14}N NMR (nuclear magnetic resonance) spectroscopy to support their model and refute that proposed by Beck, et al.[10,11]

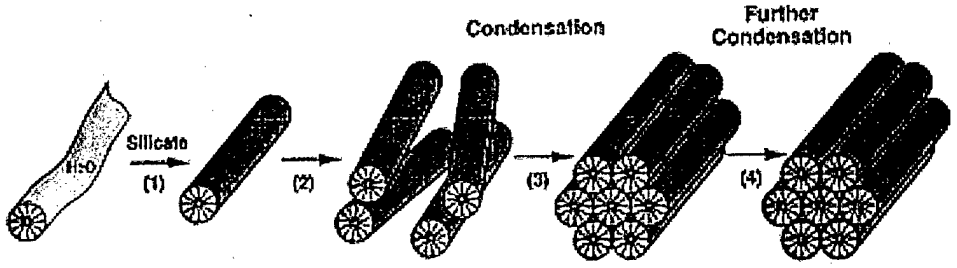

Figure 2.2: MCM-41 formation process as proposed by Davis, et al.[29] Figure taken from reference 29.

In contrast to the mesoporous silica formation process, the process of silica polymerization (generally referred to as condensation) is well understood. The following discussion is adapted from Brinker[30]. For illustrative purposes, and because it was used in the film syntheses reported in the present work, TEOS (tetraethylortho silicate) is assumed to be the silica source. A drawing of the TEOS molecule appears in Figure 2.3.

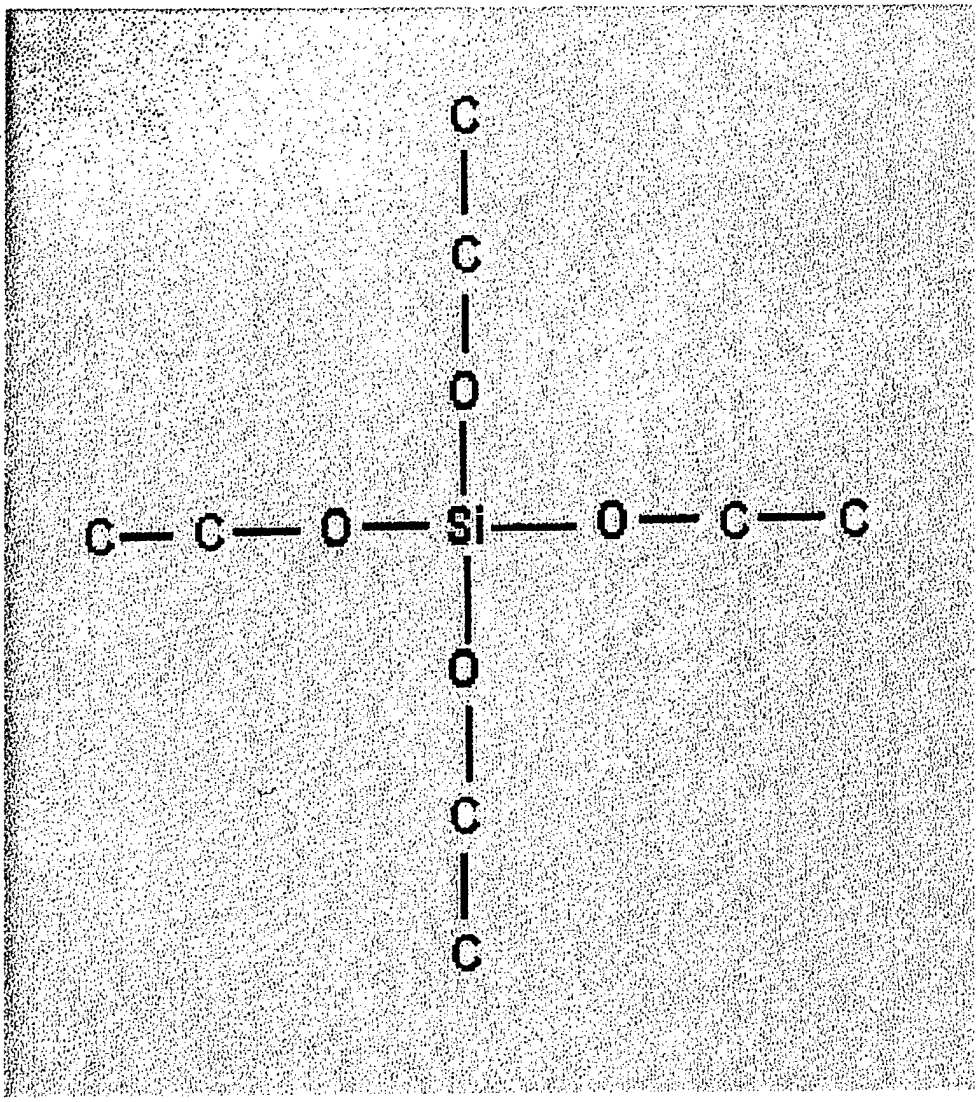

Figure 2.3: The TEOS (tetraethylorthosilicate) molecule.

Mesoporous silicates are usually synthesized in aqueous solution. The TEOS molecule reacts very easily with water in a process called hydrolysis. The hydrolysis of TEOS is diagrammed in Figure 2.4.

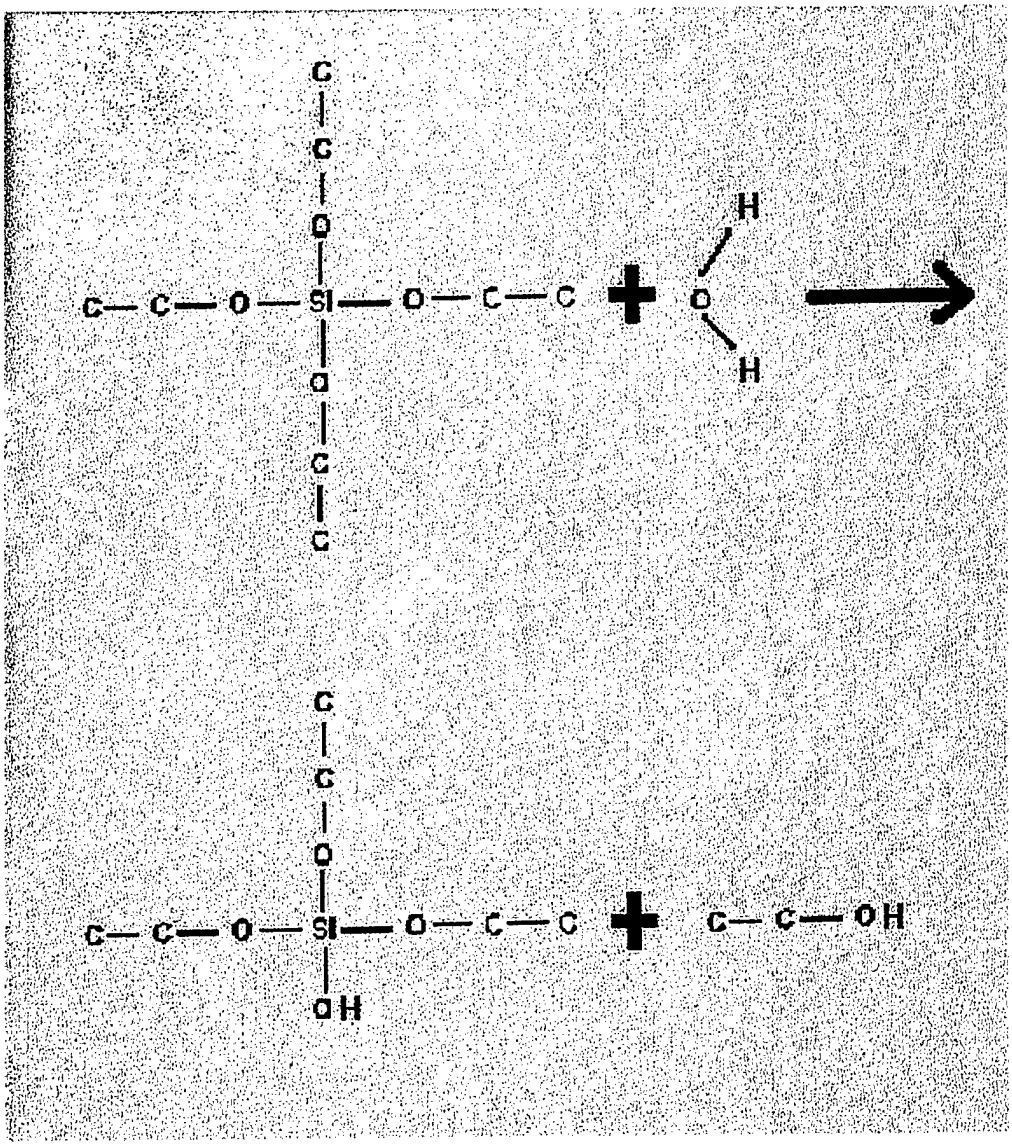

Figure 2.4: The hydrolysis of TEOS. In this example, the TEOS molecule reacts with 1 (of a possible 4) water molecules.

During hydrolysis, the silicon atom loses its ethyl groups, which go off to form ethanol, and picks up OH groups. Once hydrolysis has begun, the silica can begin

to condense. This means that Si – O – Si bonds are formed. Condensation can occur by either of two processes, depending on whether the reacting sites of both TEOS molecules have been hydrolized first or not. Figure 2.5 diagrams condensation of TEOS for the case where both reacting sites have been hydrolized. In this case, water is a byproduct. Figure 2.6 depicts condensation of TEOS molecules for the case where only one of the reacting sites has been hydrolized. In this case, ethanol is a byproduct.

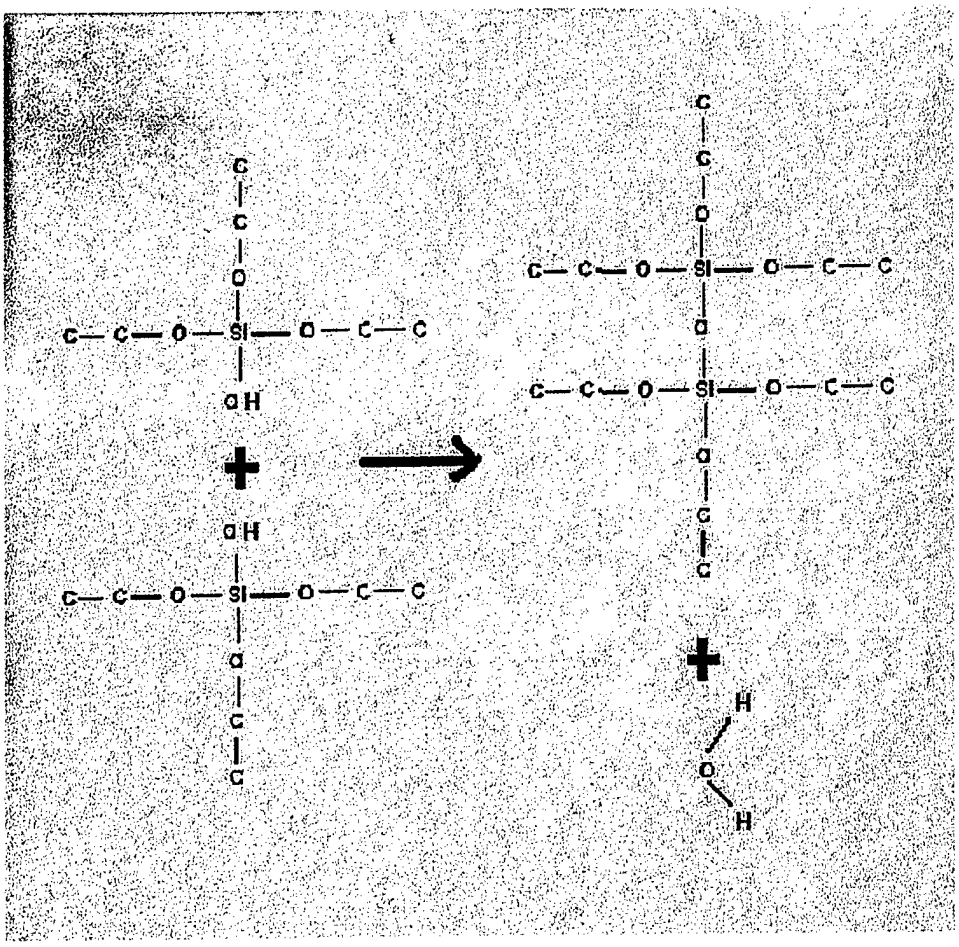

Figure 2.5: The condensation of TEOS for the case where both reacting sites have been hydrolized. In this case, water is a byproduct.

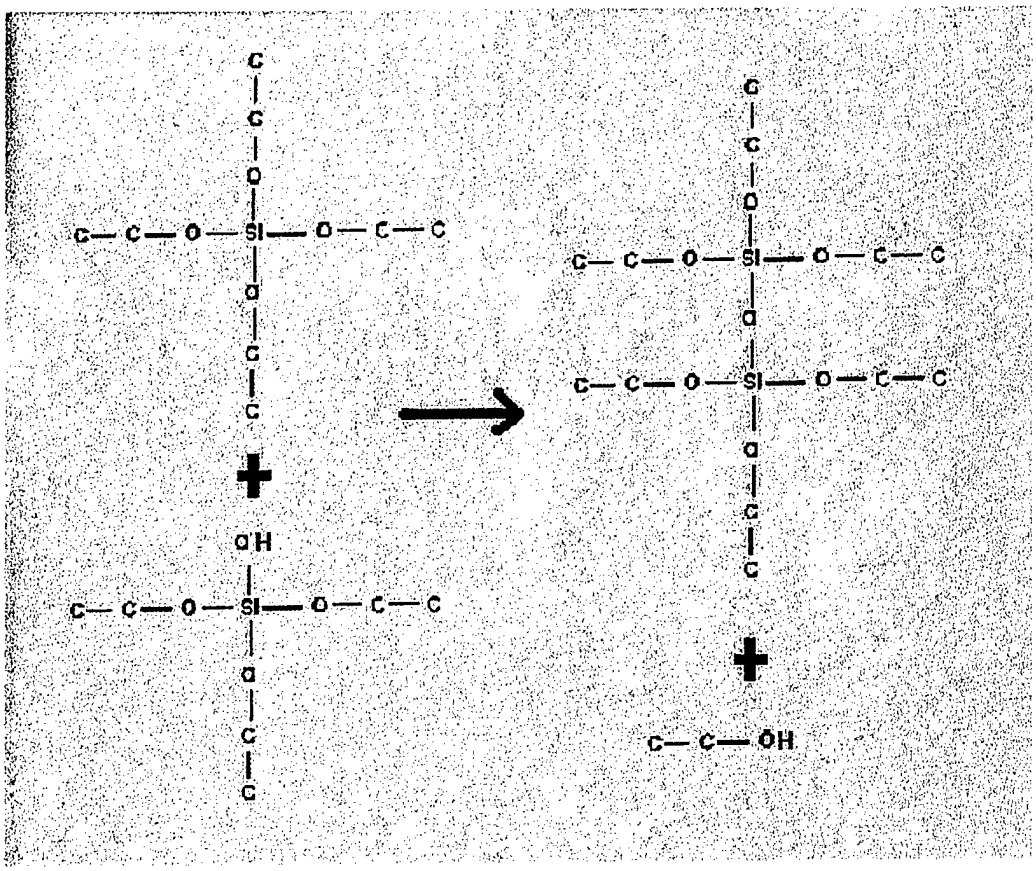

Figure 2.6: The condensation of TEOS for the case where only one of the reacting sites has been hydrolized. In this case, ethanol is a byproduct.

Condensation progresses by one or both of the ways shown above, leading to the formation of a silica network consisting of many, many Si – O – Si bonds (see Figure 2.7). Occasionally, adjacent OH sites will not condense, leading to defects in the network. Raising the temperature at which condensation occurs reduces the number of these defects. This also serves to speed the rate of silicate condensation. However, increasing the temperature of the micellar template decreases its (hexagonal or other) order. These consequences must be balanced.

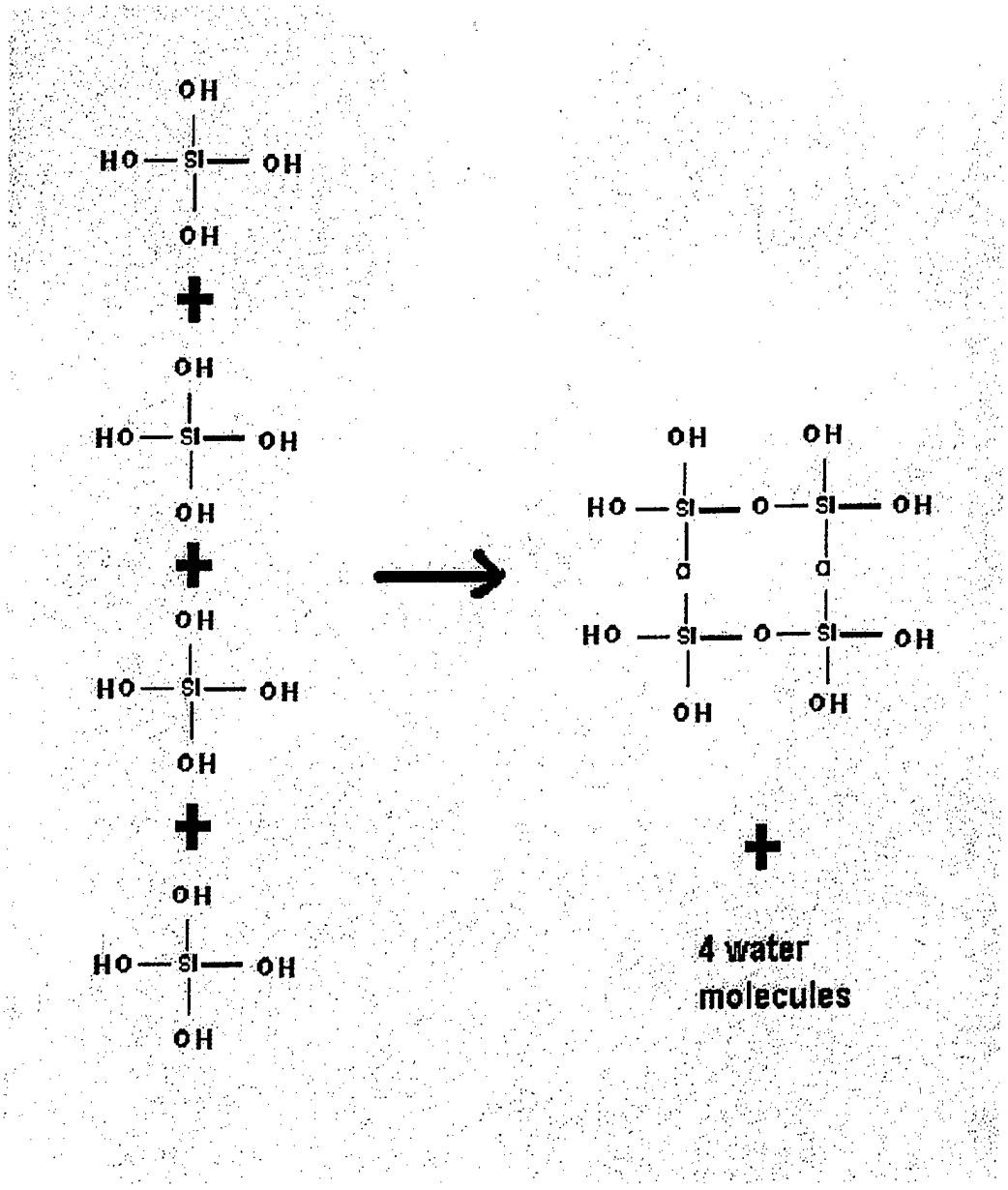

Figure 2.7: Condensation of the silicate network.

Davis et al.[29] have pointed out that condensation can occur without having formed a well ordered material. This might occur, for example, if the micellar

template were disturbed prior to condensation, or if the reactant concentrations were inappropriate or inhomogeneous in the synthesis reaction vessel. This situation is depicted in Figure 2.8, adapted from Davis, which shows condensed materials that are (A) ordered and (B) unordered. The corresponding x-ray diffraction spectra are shown as well.

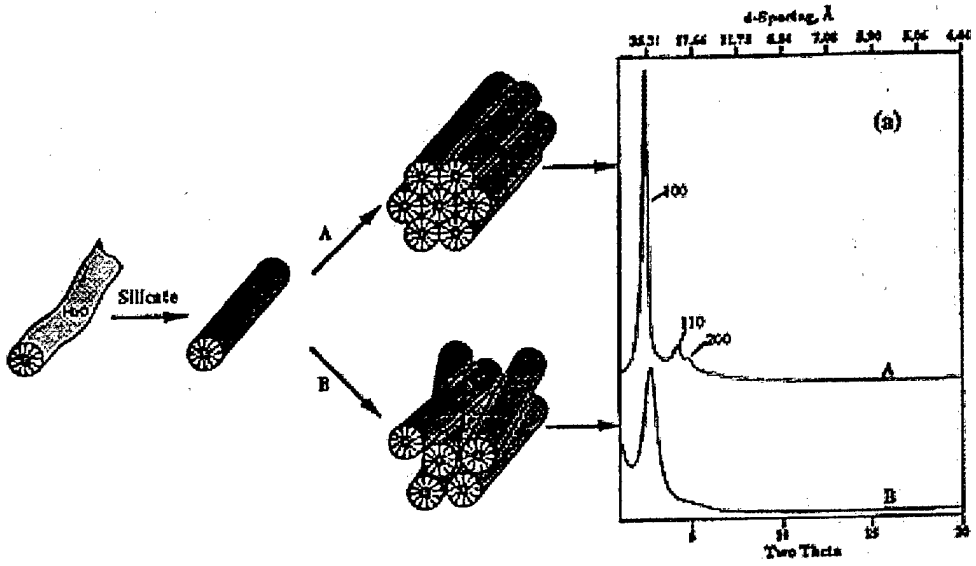

Figure 2.8: X-ray diffraction results for (A) ordered and (B) unordered condensed mesoporous silicates. Figure adapted from Davis, et al.[29]

Once the mesoporous silica has formed, and time has been allowed for silicate condensation, the material is rinsed and dried. It is then calcined (heated) under flowing air to drive out / combust the organic micellar template, leaving a hexagonal array of very uniform diameter hollow pores in silicon dioxide.

To summarize: the pore dimensions and structural phases of self assembling mesoporous silicates can be precisely controlled by the choice of templating agent and its concentration in the reaction solution. Mesoporous silicates can be highly ordered with very uniform pore diameters.

Orientation of Pores in Mesoporous Silicate Films

Several research groups have investigated the formation of mesoporous silicate films at various interfaces (air-air, air-liquid, liquid-liquid, etc.)[31-41]. The present work is concerned with the formation of films at the liquid-solid interface, where the solid is an oxidized silicon substrate. A number of researchers report formation of films on solid surfaces, such as silicon[39], glass[31,35], mica[33,35], graphite[35,36], and faujasite[32]. In all cases, the mesopores in these films were found to lie parallel to the substrate surface. Despite the attempts of many groups to orient mesopores normal to substrate surfaces, no one has yet succeeded[31-41].

The approach taken in this work was to capitalize on the tendency of the mesopores to align parallel to surfaces. D. Ast, E. Giannelis, and C. Ober proposed patterning vertical features in silicon substrates with flat walls, such as trenches and pits. By selectively altering the surface energy of the vertical surfaces on the substrate with respect to the horizontal surfaces, it was thought that the mesopores might be induced to align along the vertical surfaces. This was expected as a consequence of the system's effort to minimize free energy. It would then be necessary to further confine the pores so that their orientation within the vertical plane was controlled as desired, that is, normal to the substrate's horizontal surface. C. Ober suggested that this might be achieved by undulations in the vertical walls. It was thought that even if these undulations were several orders of magnitude

larger in size than the mesopores, that they would nevertheless align the pores vertically.

To summarize: control of surface morphology and energy was expected to lead to orientation of mesopores in mesoporous silica films.

CHAPTER THREE: SYNTHESIS OF MESOPOROUS SILICATES

Substrates

To align the mesopores perpendicular to the substrate surface, a variety of substrates were prepared and tested. These included substrates possessing various large-scale features with vertical walls, produced using optical lithography[42]. Substrates coated with hydrophobic fluoropolymer monolayers were also prepared[43,44]. The purpose of the fluoropolymer monolayers was to alter the surface energy of the substrate to induce the micellar template of the mesopores to orient along the coated surfaces. It was therefore necessary to remove these monolayers from the horizontal surfaces of the substrate, while leaving them on the vertical surfaces of patterned features. To selectively remove these coatings, an anisotropic etch procedure was developed[43]. Preliminary tests indicated that this etch procedure worked as desired[43,44]. The procedure is described below.

Silicon substrates were prepared in the following manner:

1) 3 inch Si (100) wafers were patterned by T. Dalrymple[42] using optical lithography. The pattern included 2 micron wide straight trenches spaced 2 microns apart, and various square pits, posts, and sawtooth-shaped trenches. All features had vertical walls.
2) A dry oxide ~100Å thick was deposited on these wafers by N. Nemchuk.
3) Wafers were cleaved into ~1 cm square pieces for use as substrates.
4) Substrates were RCA-cleaned by N. Donnelly and the author. This consisted of:
   a) A 10 minute base bath (1 part NH_4OH, 1 part H_2O_2, and 5 parts H_2O) at 65° C.
   b) A 4 minute rinse in deionized water.
   c) A 10 minute acid bath (1 part HCl, 1 part H_2O_2, and 5 parts H_2O) at 65° C.

d) A 4 minute rinse in deionized water.

e) Blow drying with N_2.

f) The typical final HF step was skipped, in order to preserve the oxide layer.

5) The substrates were coated with a hydrophobic fluorinated polymer monolayer (1H, 1H, 2H, 2H-perfluorodecyltrichlorosilane) by N. Donnelly[44], following the vapor priming procedure developed by Y. Takamura[43].

6) Half of the substrates were ion milled by N. Donnelly[44] to remove the fluoropolymer from the horizontal surfaces of these substrates.

7) The remaining substrates were used as is, i.e. all surfaces completely coated with fluoropolymer.

Preparation from Basic Solution

Mesoporous silicates were synthesized under a variety of reaction conditions, resulting in the production of high quality bulk MCM-41. In this bulk form, MCM-41 is a powder that precipitates from solution as the synthesis reaction progresses. This powder is the typical reaction product of a basic synthesis preparation. The best results were obtained with the following process:

Into a polypropylene bottle were added while stirring the following, in the order given:

1) 201.05 g of cetyltrimethylammonium chloride (CTACl), 25 wt% in aqueous solution.

2) 153.86 g of deionized water.

3) 56.38 g of sodium silicate solution

4) 17.06 g of sulfuric acid (H_2SO_4) (added slowly).

This mixture was allowed to sit for 30 minutes, after which 115 drops of 50 wt% sulfuric acid were added while stirring until the pH of the mixture was

lowered to 11. The mixture was capped and allowed to sit at room temperature for 48 hours. At room temperature, micellar order is relatively stable, while silicate polymerization progresses very slowly. Conversely, at higher temperatures, silicate polymerization is more rapid, but the micelles become disordered unless "frozen" in place by the silicate network. C. Ober suggested the room temperature step to allow polymerization to begin with maximum ordering of the micelles. The mixture was then placed in an oil bath that had previously been heated to 88° C, and the cap loosened slightly. After 24 hours, the pH was measured to be 12, and 61 drops of 50 wt% sulfuric acid were added to bring the pH back down to 11, after the method of K. Edler[45,46], who studied MCM-41 quality as a function of synthesis pH. After 24 more hours, the pH was measured to be 11.5, and 20 drops of 50 wt% sulfuric acid were added to bring the pH down to 11. The mixture remained at elevated temperature for 48 more hours. See Table 3.1.

Table 3.1: Typical Mesoporous Silica Basic Synthesis Conditions

Elapsed Time (days)	Temperature of Mix (°C)	pH as Measured	50 wt% H_2SO_4 Added (drops)	pH after Adding Acid
0	23	11	0	11
1	23	11	0	11
2	23	11	0	11
3	80	12	61	11
4	80	11.5	20	11
5	84	11	0	11
6	79	11	0	11

It should be noted that the temperatures in Table 3.1 are those of the reaction mixture, not the oil in the oil bath. The oil temperatures were somewhat higher. Samples were from batch A05.bxx.

The mixture remained at an elevated temperature as indicated in Table 3.1 for 4 days, after which it was removed from the oil bath and allowed to cool to room temperature naturally. The MCM-41 precipitate was then washed with deionized water in a Buechner funnel and allowed to dry naturally in a petri dish. A sample of this as-synthesized MCM-41 was taken for x-ray diffraction, and the rest was calcined to remove the organic template.

The typical calcination procedure for bulk MCM-41 was to place the powder in a ceramic boat in the center of a tube furnace with a constant supply of flowing air. The furnace was heated from room temperature to 600° C at 1° C per hour. The temperature was held at 600° C for 6 hours, then cooled to room temperature at approximately 1° C per hour.

The presence in both the uncalcined and calcined bulk MCM-41 powders of hexagonally ordered, uniform diameter mesopores was confirmed by x-ray diffraction (see Chapter Five). The presence of these pores in the calcined sample was further confirmed by TEM (see Chapter Four).

Attempts were made to produce films of MCM-41 on silicon substrates from basic synthesis. These attempts resulted only in precipitating powder onto the substrate, rather than growing films by nucleation at the solution-substrate interface. These powders usually did not adhere well to the substrate and were often unstable to calcination, as determined by no evidence of structure in post-calcination x-ray diffraction experiments. It is likely that condensation of the silicate network was too rapid in basic synthesis to allow for the formation of films.

Preparation from Acidic Solution

In order to obtain MCM-41 films on silicon substrates, synthesis of MCM-41 under acidic conditions was investigated. The best results were obtained with the process outlined below.

Mesoporous silica was synthesized using the recipe of Yang, et al.[33] as a starting point. Into a polypropylene bottle were added without stirring the following, in the order given:

1) 44.69 g deionized water.
2) 25.76 g hydrochloric acid (HCl), 37 wt% aqueous solution.
3) 5.06 g CTACl, 25 wt% aqueous solution.

This mixture was stirred for 10 minutes and then set aside for 70 minutes. 1.26 g of tetraethylorthosilicate (TEOS) was then added, and the mixture was stirred for 4 minutes.

The mixture was then poured into two separate polypropylene jars, into which were placed plastic racks to hold the substrates. The level of the solution in these jars was such that it just reached the top of the racks. Substrates were placed upside down on the racks, so that their patterned and coated surfaces were held in contact with the solution. The substrates were prepared as described in the section entitled "Substrates" at the beginning of this chapter. One jar held ion milled substrates and the other held non-ion milled substrates. The jars were tightly capped. These jars were placed in separate oil baths, whose temperatures had been previously elevated to about 85° C. Samples consisting of substrates coated with mesoporous silica were then pulled from the jars containing the reaction mixtures as shown in Table 3.2 below.

Table 3.2: Mesoporous Silica Film Preparation from Acidic Solution

Sample Number	Elapsed Time in Reaction Mixture (hours)	Substrate Hydrophobic Coating	Temperature at Exit (°C)
1	1	Not milled	80
2	1	Milled	72
3	2.2	Not milled	67
4	2.2	Milled	61
5	4	Not milled	52
6	4	Milled	58
7	7.8	Not milled	64
8	7.7	Milled	58
9	24	Not milled	68
10	24	Milled	62
11	63.5	Not milled	22*
12	63.5	Milled	24*
13	63.5	Milled	24*

* The temperature was allowed to ramp down naturally to room temperature once 48 hours had elapsed. Samples B03.wxx.

Special care was taken on removing samples from the jars to ensure that oil from the oil bath did not contaminate the reaction mixtures, and that the hot acidic solutions did not spill. Samples were allowed to dry naturally (this is a very slow

process, they remain tacky for days without calcination, and structural/ordering changes can occur in the film during this time).

The synthesis process just outlined produced films with the best temperature stability. However, all films grown were unstable at typical calcination conditions of 600° C. Results concerning temperature stability are discussed in Chapter Five in the section entitled "Theta-Two Theta Measurements at Elevated Temperatures".

CHAPTER FOUR: CHARACTERIZATION OF MESOPOROUS SILICATES BY MICROSCOPY

Transmission Electron Microscopy (TEM)

TEM images were obtained of bulk MCM-41 powder prepared by basic synthesis. These images confirm the presence of hexagonally ordered, uniform diameter mesopores. Pore diameter is of the order of 25Å, as is expected for the particular surfactant (CTACl) used in the synthesis of this sample. Figure 4.1 shows a close-up view of pores in a particle that is roughly 150 nm long. Figure 4.2 shows the entire particle.

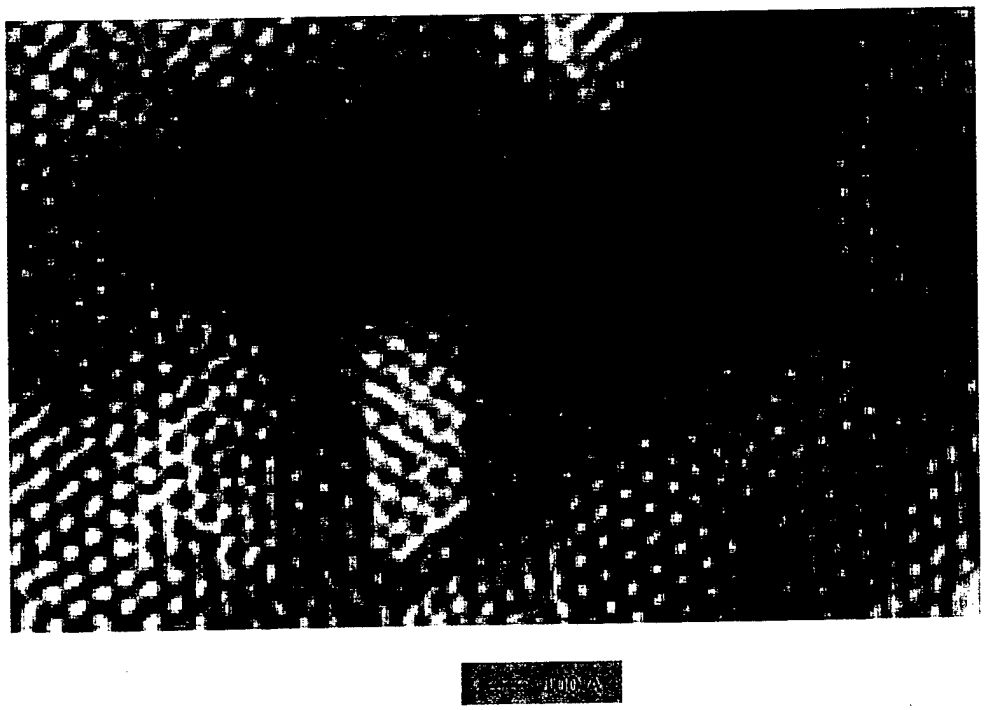

Figure 4.1: TEM micrograph of MCM-41 mesopores in a particle prepared by basic synthesis. Sample A05.b5c.

Figure 4.2: TEM micrograph of the entire particle of Figure 4.1. Sample A05.b5c.

The TEM specimens of bulk MCM-41 powders in Figures 4.1 and 4.2 were prepared by suspending MCM-41 particles in solvent, depositing on holey carbon film, and evaporating the solvent.

TEM specimens of mesoporous silica films grown by acidic synthesis on Si/SiO_2 substrates were prepared by tripod polishing. There is a significant probability that this process damaged the film samples. TEM images obtained from such a sample are shown in Figures 4.3 and 4.4. Mesopores are observed, but hexagonal ordering is not observed.

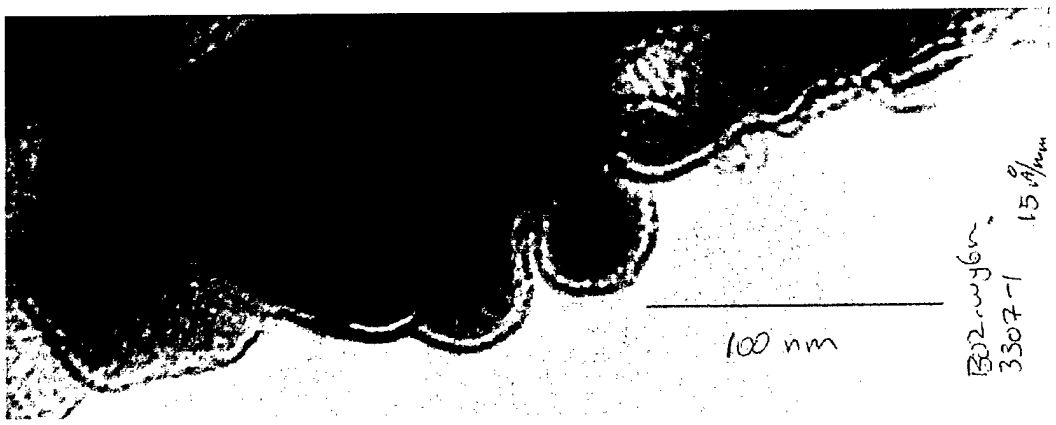

Figure 4.3: TEM micrograph of a mesoporous silica film grown by acidic synthesis on an Si/SiO2 substrate. Sample B02.wy6n.

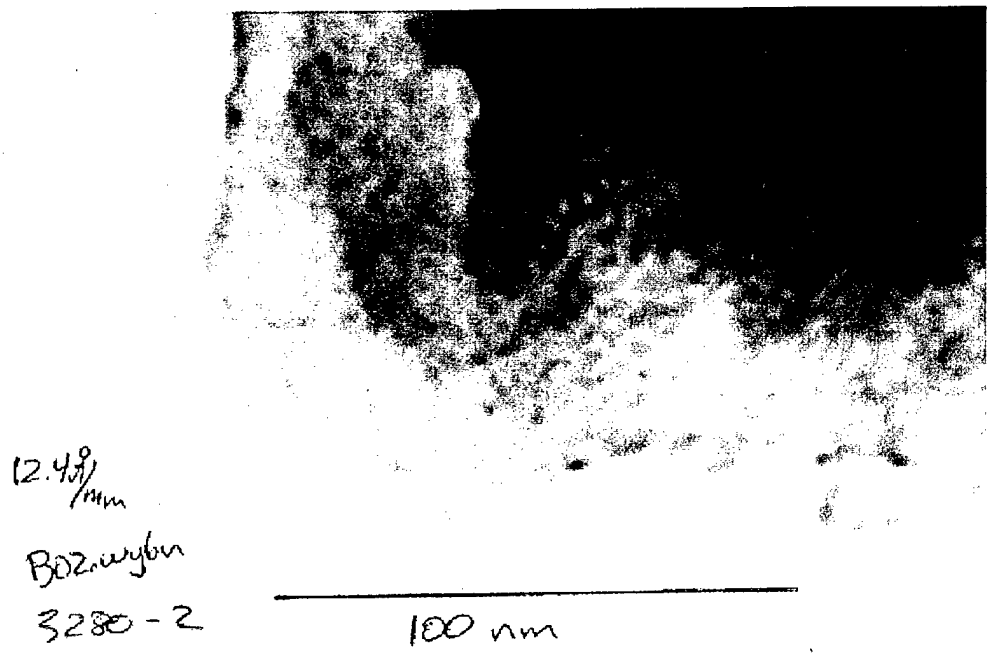

Figure 4.4: TEM micrograph of a mesoporous silica film grown by acidic synthesis on an Si/SiO2 substrate. Sample B02.wy6n.

The TEM images in Figures 4.1 through 4.4 were obtained by N. Jiang of the CCMR on a JEOL instrument at an operating voltage of ~120 kV. TEM specimen preparation was also done by N. Jiang.

Scanning Electron Microscopy (SEM)

SEM images were obtained of MCM-41 deposited on Si/SiO_2 substrates by precipitation during basic synthesis. Figure 4.5 shows MCM-41 particles lodged in and around a trench etched in the substrate. The sample had been calcined.

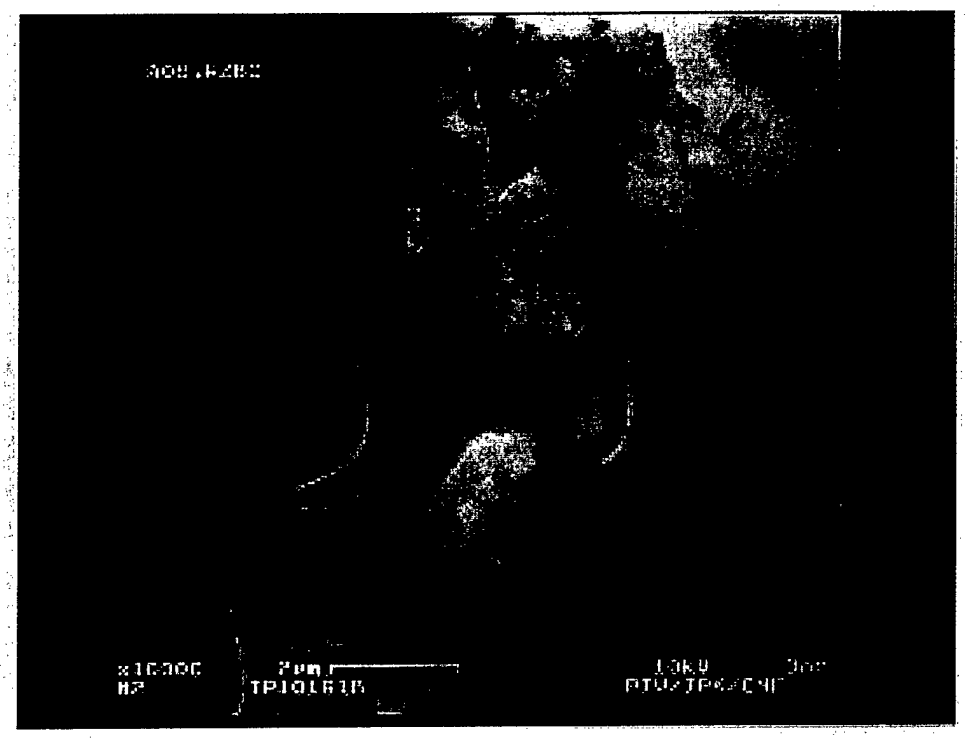

Figure 4.5: SEM micrograph of a sample showing MCM-41 particles deposited in a trench. Sample A06.w28c.

Figure 4.6 shows a close-up view of uncalcined MCM-41 particles deposited in a trench during basic synthesis on a sample similar to the sample shown in Figure 4.5.

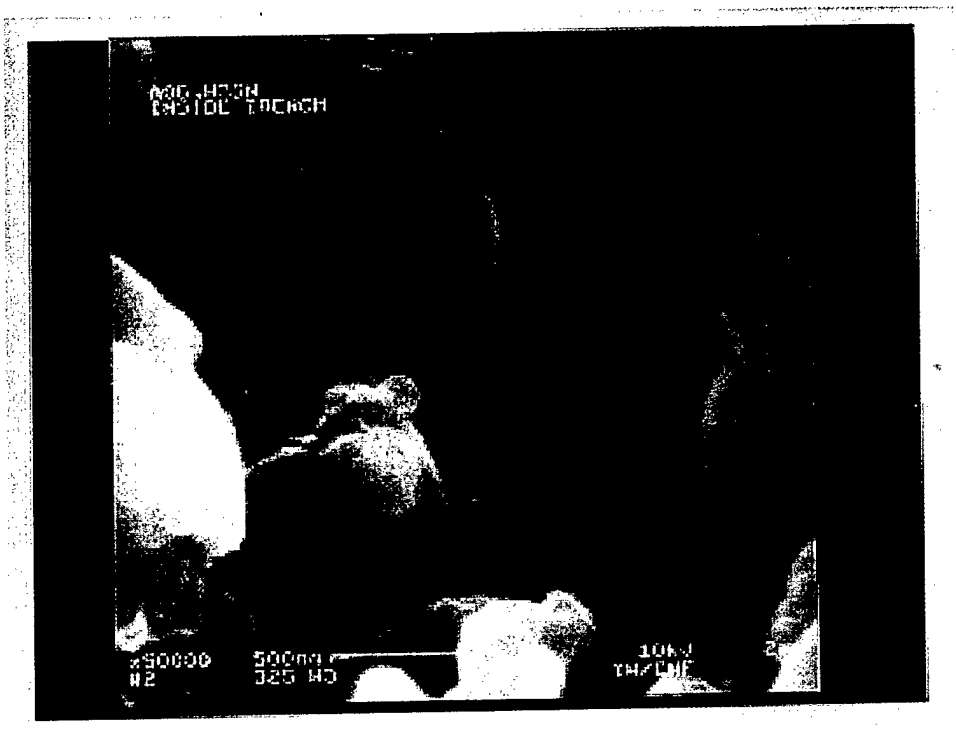

Figure 4.6: SEM micrograph of a sample showing close-up view of MCM-41 particles in a trench. Sample A06.w36n.

Figure 4.7 shows mesoporous silica particles deposited on an Si/SiO_2 substrate during acidic synthesis. The substrate was exposed to the synthesis gel for 6 hours 40 minutes at 80° C.

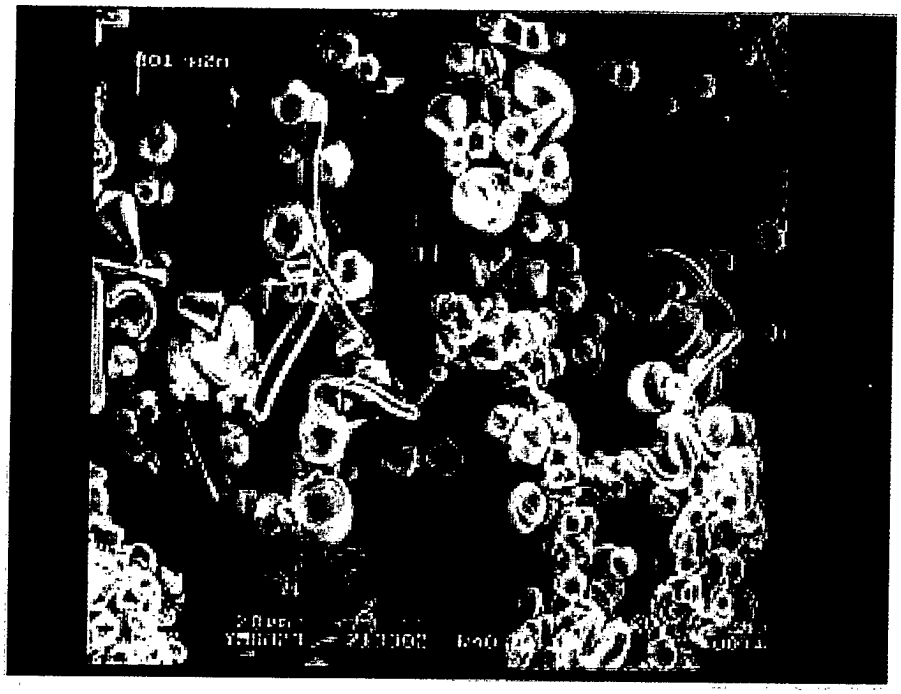

Figure 4.7: SEM micrograph of mesoporous silica particles from acidic synthesis. Sample B01.w2n.

Figure 4.8 shows a close-up view of some of the particles shown in Figure 4.7.

Figure 4.8: SEM micrograph of mesoporous silica particles from acidic synthesis. Sample B01.w2n.

Figure 4.9 shows mesoporous silica film-like structure deposited on the surface of a patterned substrate during acidic synthesis. The substrate was exposed to the synthesis gel for 26 hours 10 minutes at 80° C.

Figure 4.9: SEM micrograph of mesoporous silica film from acidic synthesis. Sample B01.w3n.

Figures 4.10, 4.11, and 4.12 show a mesoporous silica film grown by acidic synthesis on a trench-patterned Si/SiO_2 substrate. The film cracked upon drying. Small triangular pits are evident in Figure 4.11, which appear to occur where different growth fronts in the film meet each other. Figure 4.12 shows a close-up view of one of the triangular pits. The substrate was exposed to the synthesis gel for 5 hours 20 minutes at 80° C.

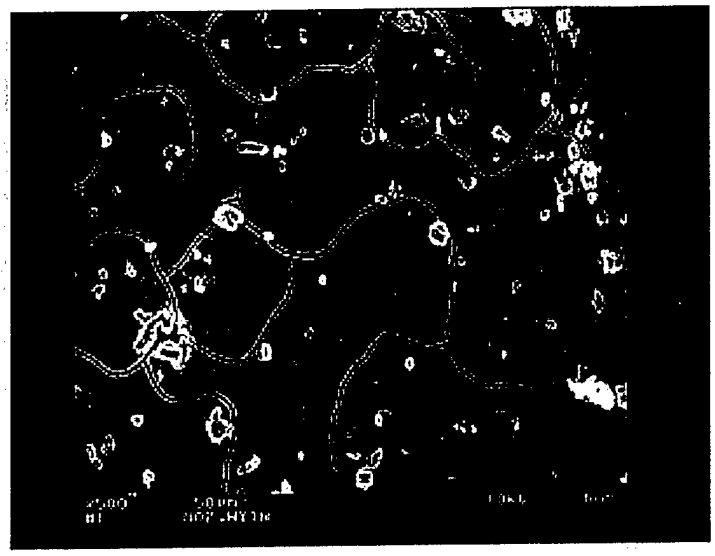

Figure 4.10: SEM micrograph of a mesoporous silica film grown from acidic synthesis on an Si/SiO_2 substrate. Sample B02.wy1n.

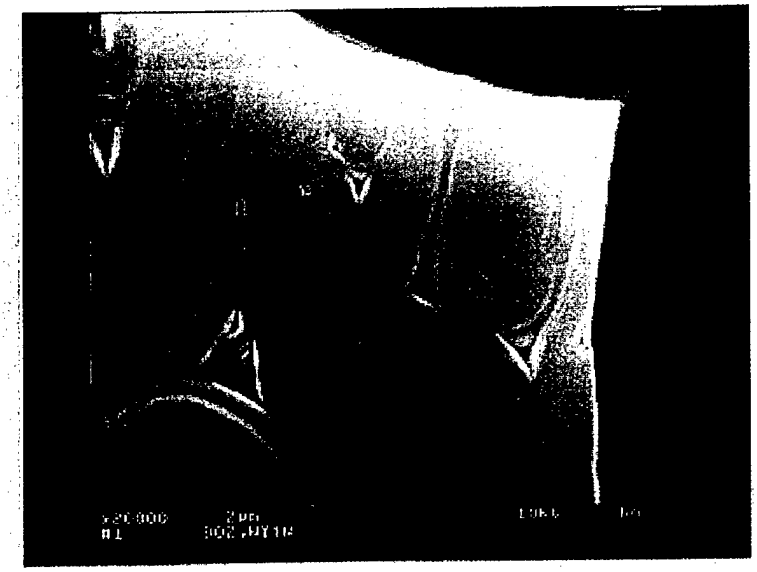

Figure 4.11: SEM micrograph of a mesoporous silica film grown from acidic synthesis on an Si/SiO_2 substrate. Sample B02.wy1n.

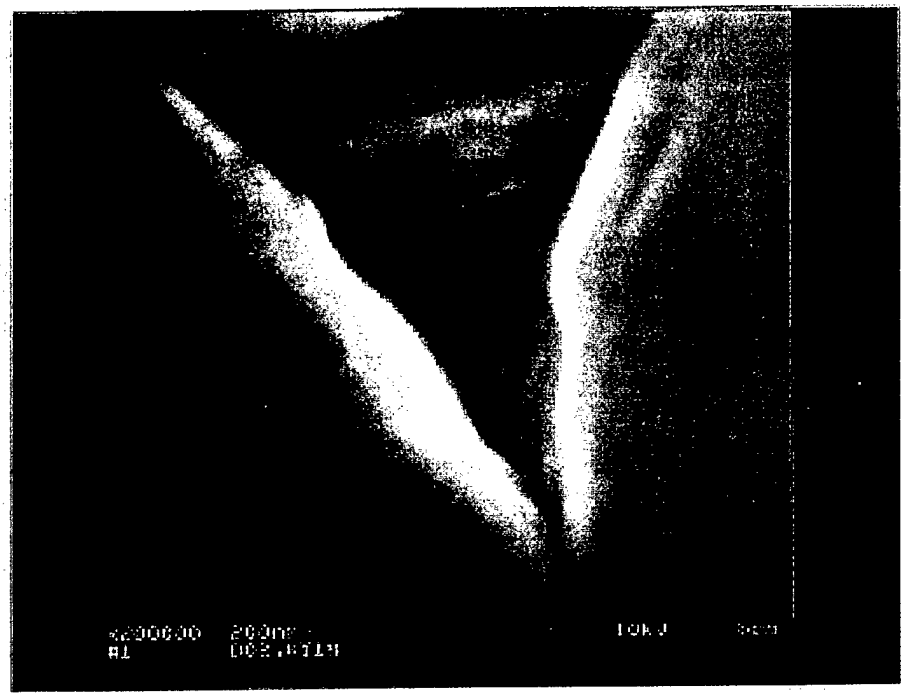

Figure 4.12: SEM micrograph of a mesoporous silica film grown from acidic synthesis on an Si/SiO_2 substrate. Sample B02.wy1n.

Mesoporous silica films grown on silicon substrates were imaged with a high-resolution field emission SEM. This instrument was operated by G. Nagy of the Cornell Nanofabrication Facility. We were unable to observe the presence of internal structure in the deposited film. However, we were able to observe the presence of internal structure (see Figure 4.14) in a particle of mesoporous silica that had grown or become lodged upon a mesoporous silica film deposited on silicon (see Figure 4.13). We were unable to resolve this structure on small enough

length scales to observe the actual 25Å pores. The substrate was exposed to the synthesis gel for 24 hours at 68° C, after initially being heated to 85° C.

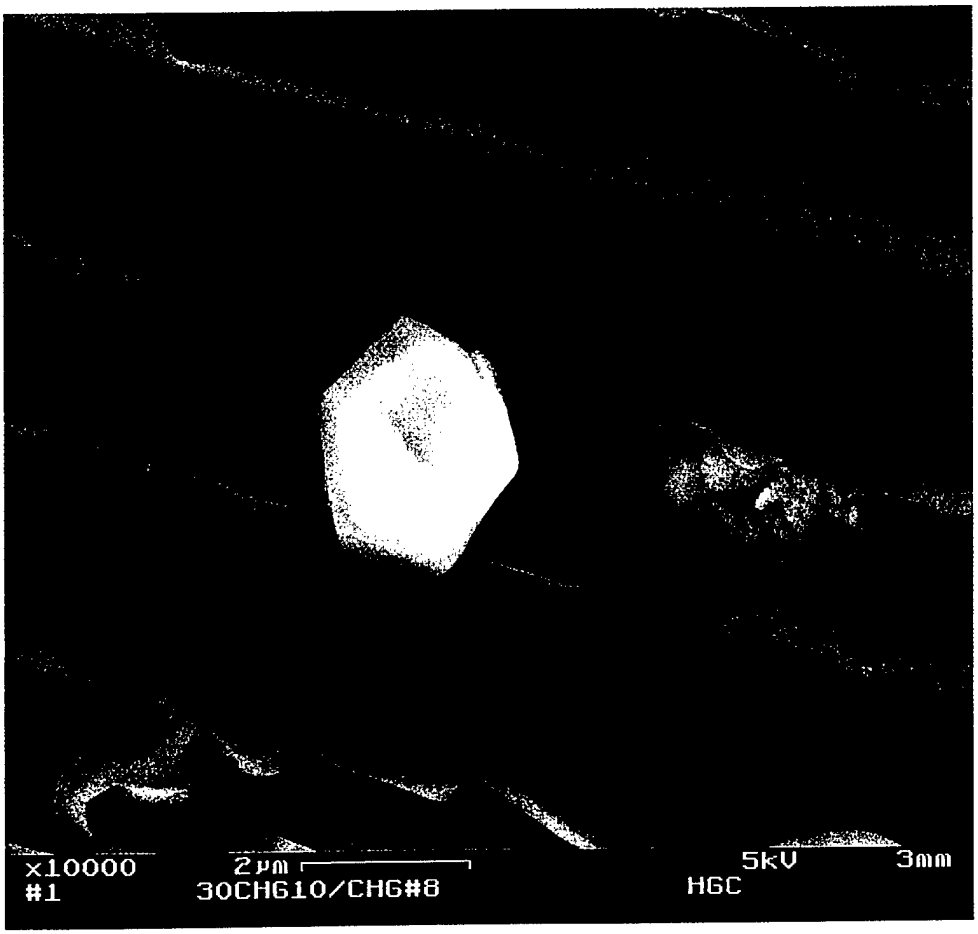

Figure 4.13: SEM micrograph of a hexagonally shaped mesoporous silica particle on a mesoporous silica film. The film is adhered to 2 µm wide lines patterned on a silicon substrate. Sample B03.w9n.

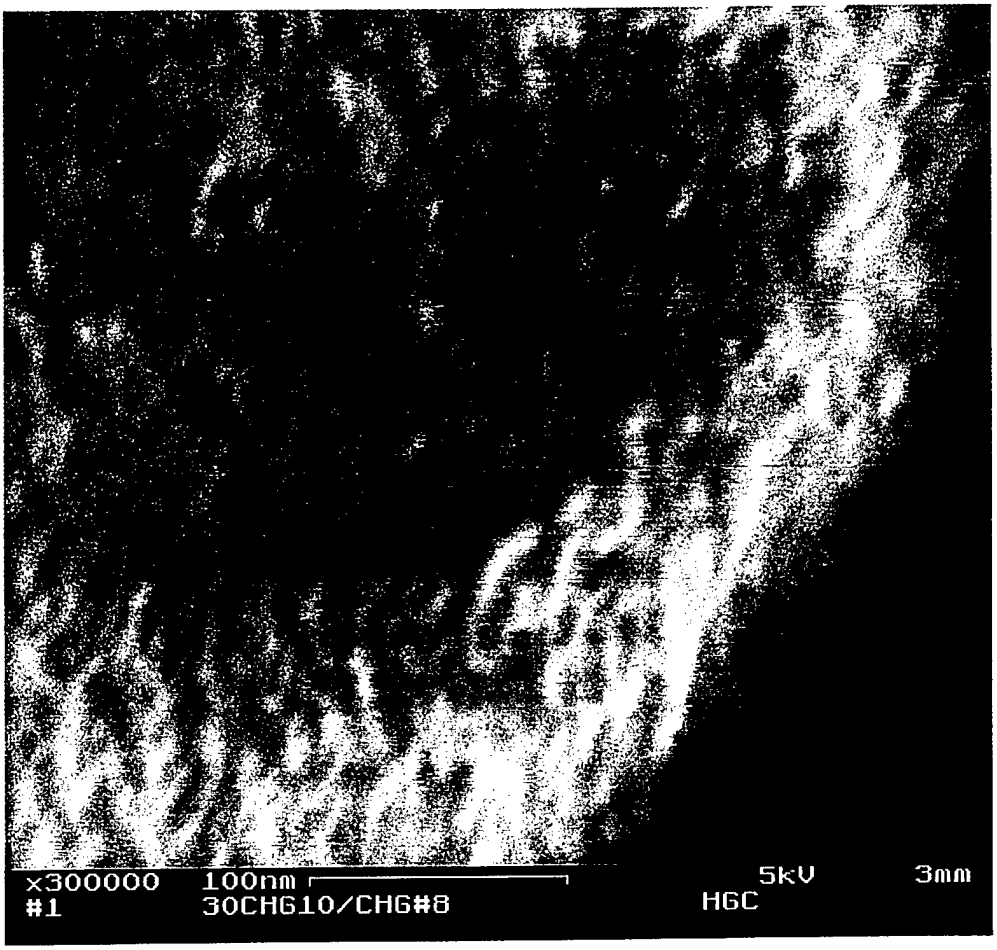

Figure 4.14: SEM micrograph showing a close-up view of the mesoporous silica particle shown in Figure 4.13. Sample B03.w9n.

Atomic Force Microscopy (AFM)

Two test samples of unoriented mesoporous silica on silicon substrates were prepared for AFM measurements. One sample consisted of a typical mesoporous silica film grown on an Si/SiO_2 substrate, as described in Chapter Three. The other sample was prepared using MCM-41 powder affixed to a silicon substrate with a spin-on glass (Allied Signal Accuglass® 111). The powder was randomly oriented,

therefore the cylindrical mesopores should be present with their symmetry axes in random orientations. These samples were sent to Hewlett-Packard Laboratories (HP Labs) for AFM studies.

Spin-on glass (SOG) samples were prepared as follows. The SOG was deposited on 1 cm square Si/SiO_2 substrates by spin-coating at 2500 rpm for 8 seconds, or at 2000 rpm for 6 seconds. MCM-41 bulk powder (the presence of hexagonal, uniform mesopores was previously confirmed by x-ray diffraction and TEM) was placed on top of the still wet SOG film. The samples were then baked on a hotplate at 90° C for 60 seconds. The samples were then cured in an oven at 425° C for 1 hour under flowing air. The oven was ramped up and down at approximately 1° C per minute. The finished samples were characterized by theta-two theta x-ray diffraction, as described in Chapter Five, as well as optical microscopy, which confirmed that there was no damage to the MCM-41 during SOG processing.

AFM studies of the two unoriented mesoporous silica samples were conducted at HP Labs by Dr. T. Kamins. Imaging was difficult because of the surface roughness of both samples. Figure 4.15 is an image taken of a mesoporous silica film grown on an Si/SiO_2 substrate. It shows dots ~30 Å in diameter, which is the right diameter for vertical MCM-41 pores. These dots appear to be ordered in rows or columns, but hexagonal ordering is not observed. Depending on how one interprets the lower (dark) regions between the elevated (light) dots, the dot spacing is either (a) as expected for MCM-41 pores, if the dark regions are "short" pores, or (b) twice that expected for MCM-41 pores, if the dark regions are (thick) walls between pores. TEM images of comparable mesoporous silica films (see Figures 4.3 and 4.4) show pores in patterns similar to the dots here observed by AFM. That is, there are wavy rows of pores, and varying wall thicknesses, but no hexagonal

ordering. This result is consistent with the material being poorly formed MCM-41. X-ray diffraction results for these and comparable films are also consistent with poorly formed MCM-41.

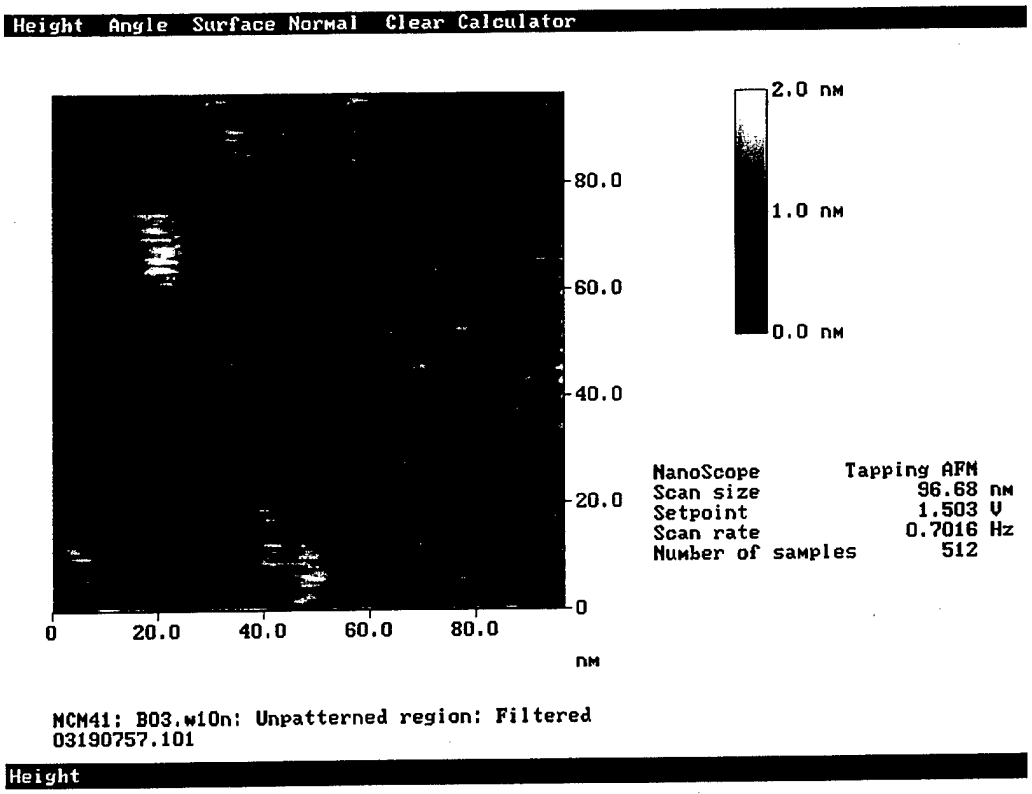

Figure 4.15: AFM image of a mesoporous silica film grown on an Si/SiO_2 substrate, showing what may be vertical pores. Sample B03.w10n.

Figure 4.16 is an image taken of the same mesoporous silica film imaged in Figure 4.15, but from a different region of the sample. Terrace-like structures are observed along the region of greatest vertical contrast. These terraces are ~30 Å

wide, which is about the right width for MCM-41 pores. These terraces could be horizontal pores.

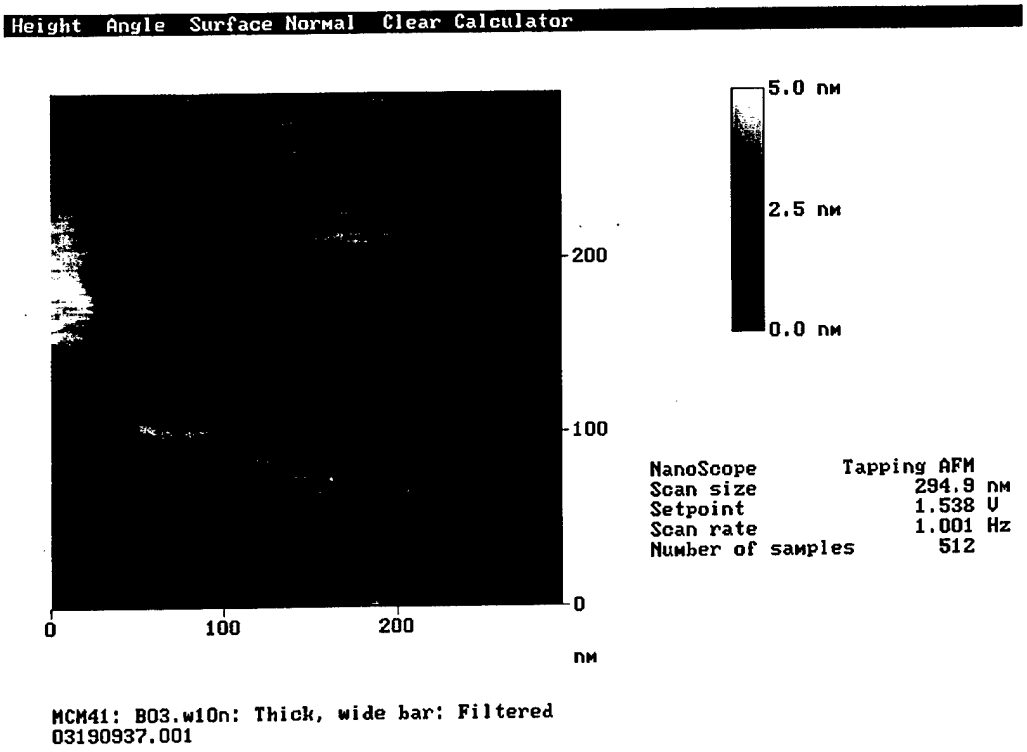

Figure 4.16: AFM image of a mesoporous silica film grown on an Si/SiO_2 substrate, showing what may be horizontal pores. Sample B03.w10n.

Figure 4.17 shows an image of an MCM-41 particle affixed to an Si/SiO_2 substrate with spin-on glass, by the procedure described above. Rod-like structures ~250 Å in diameter and ~800 Å long are visible. 250 Å is much too big for a single pore, but, as was suggested by Dr. Kamins, these rods may actually be bundles of

pores. However, individual pores could not be resolved by the AFM. Imaging this sample was particularly difficult because of surface roughness.

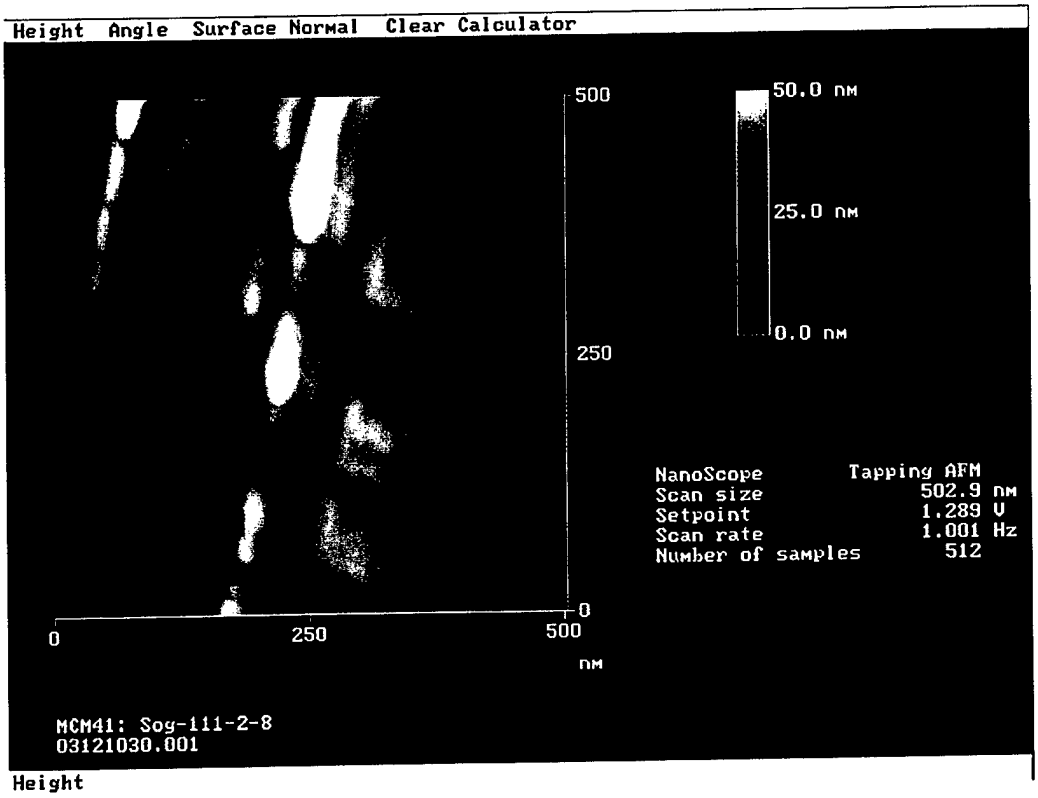

Figure 4.17: AFM image of an MCM-41 particle affixed to a substrate with spin-on glass. Sample SOG111-2-8.

CHAPTER FIVE: CHARACTERIZATION OF MESOPOROUS SILICATES BY X-RAY DIFFRACTION

Theta-Two Theta Measurements at Room Temperature

X-ray diffraction experiments utilizing a theta-two theta diffractometer were carried out on all bulk powder and all film mesoporous silica samples synthesized. Ordering in these samples was thus elucidated. Figure 5.1 shows the diffraction spectrum of a typical high-quality MCM-41 bulk sample prior to calcination. In this x-ray diffraction spectrum, as in those that follow (Figures 5.2 – 5.18), intensity in units of counts per second is plotted as a function of 2-theta in units of degrees. The sample in Figure 5.1 was prepared by basic synthesis, as described in Chapter Three.

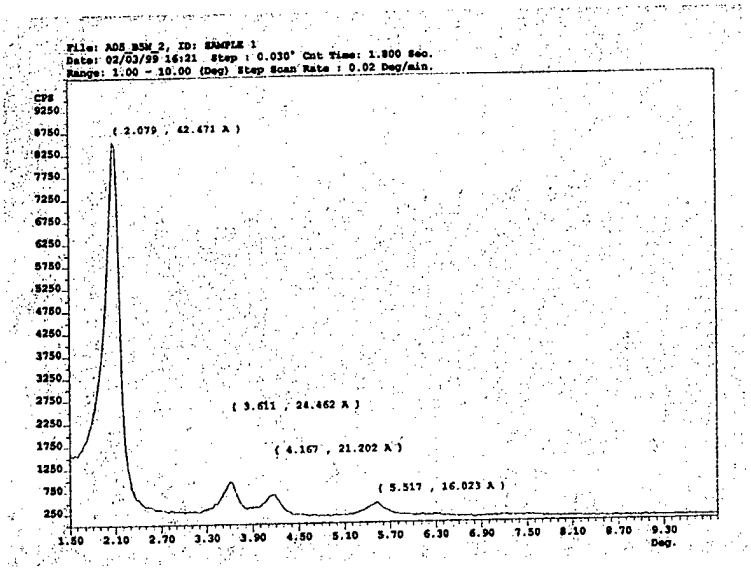

Figure 5.1: X-ray diffraction spectrum from a bulk MCM-41 sample, obtained prior to calcination. Intensity in counts/sec is plotted against 2-theta in degrees. Sample A05.b5n.

Figure 5.2 shows the diffraction spectrum from the same bulk sample shown in Figure 5.1, but after calcination at 600° C. Following calcination, there is a lattice contraction of about 8.5 %. The sample is highly ordered, and the structure remains well defined. The four peaks at 2.27°, 3.88°, 4.47°, and 5.88° 2-theta were indexed to a hexagonal unit cell and represent (100), (110), (200), and (210) planes respectively. The post-calcination (100) d-spacing of 38.9 Å is consistent with TEM results for the same sample (see Figures 4.1 and 4.2).

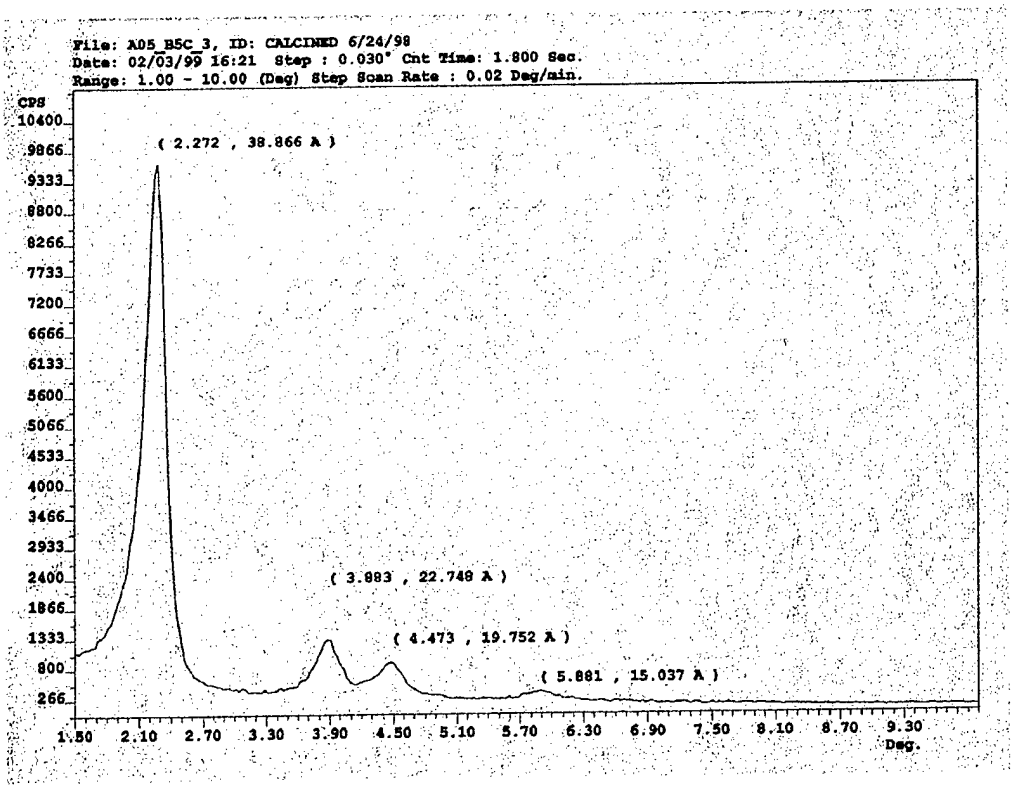

Figure 5.2: X-ray diffraction spectrum from a bulk MCM-41 sample, obtained after calcination. Sample A05.b5c.

Figures 5.3 and 5.4 show the diffraction spectrum of a typical mesoporous silica film sample prior to calcination. The sample was prepared by acidic synthesis, as described in Chapter Three. Three of the four diffraction peaks that normally signify the presence of hexagonally ordered MCM-41 (those at 3.8°, 4.5°, and 4.9° 2-theta, see close-up in Figure 5.4) are not nearly as intense with respect to the first peak as is observed in bulk samples. The presence of the peaks at 2.84°, 5.58° and 8.33° 2-theta indicates the presence of a lamellar phase in addition to the hexagonal phase. It is not known whether this lamellar phase consists of surfactant only, or whether it is surfactant-templated silica.

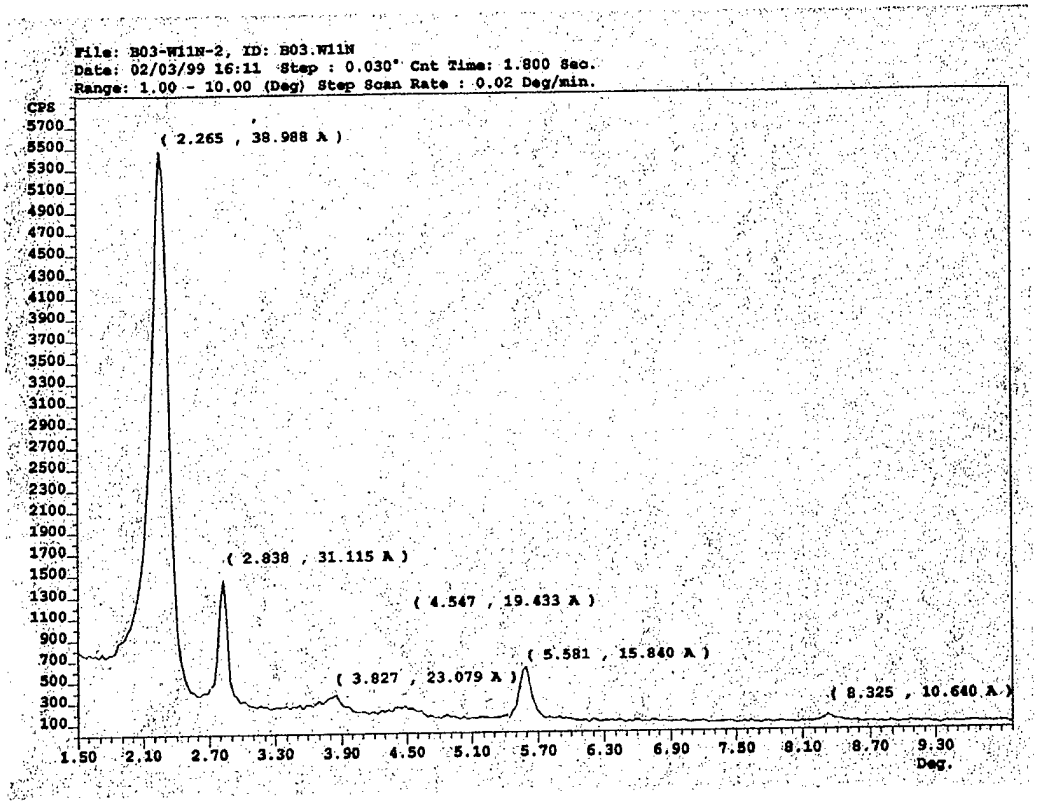

Figure 5.3: X-ray diffraction spectrum from a mesoporous silica film sample, obtained prior to calcination. Substrate was not ion milled. Sample B03.w11n.

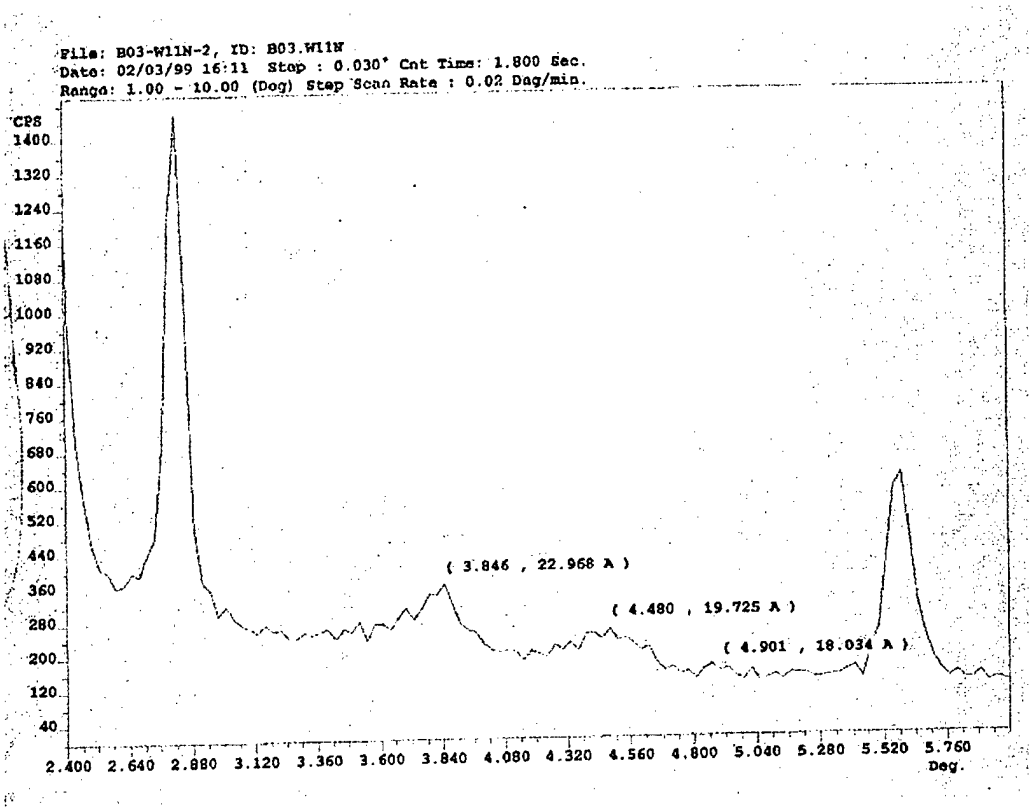

Figure 5.4: Close-up of the range 2.4° to 6.0° 2-theta shown in Figure 5.3. Sample B03.w11n.

Figure 5.5 shows the diffraction spectrum from a film sample similar to that shown in Figure 5.3, but after calcination at 650° C for several hours. Order has largely been lost. This phenomenon will be discussed in detail later in this chapter in the section entitled "Theta-two theta Measurements at Elevated Temperatures".

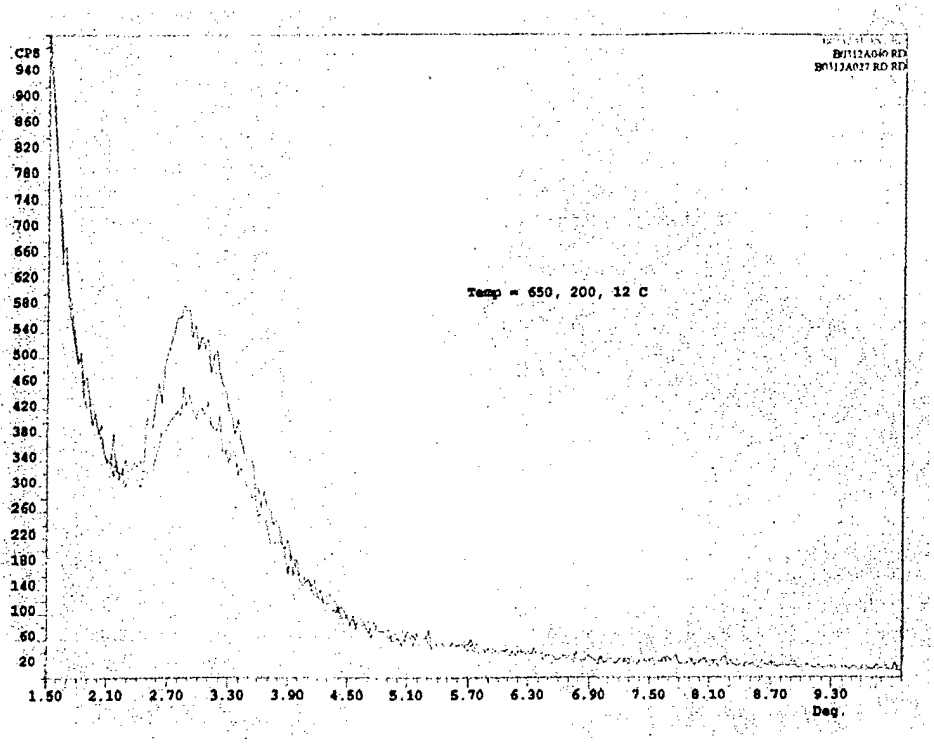

Figure 5.5: X-ray diffraction spectrum from a mesoporous silica film sample, obtained after calcination at 650° C for several hours. Sample B03.w12.

As discussed in Chapter Three and shown in Table 3.2, mesoporous silica films were grown on substrates that had one of two types of coating preparation:

1) fluoropolymer monolayer on all surfaces of the substrate (not ion milled)
2) fluoropolymer monolayer on all surfaces initially, then ion milled to remove the fluoropolymer from the horizontal surfaces of the substrate.

X-ray diffraction results for mesoporous silica films grown on these two types of substrates differed. Figure 5.6, with a close-up in Figure 5.7, shows the x-ray diffraction spectrum from a mesoporous silica film grown on a substrate that had been ion milled. Compare these results to Figure 5.3 (and the corresponding close-

up in Figure 5.4), which shows a film sample synthesized in the same batch as the sample in Figures 5.6 and 5.7, but grown on a substrate that was not ion milled. In the close-up of Figure 5.4, the MCM-41 peaks at 3.85° and 4.48° 2-theta, corresponding to the (110) and (200) planes respectively, have relative intensities consistent with typical MCM-41 bulk samples. That is, the (110) reflection is more intense than the (200) reflection. However, in the close-up of Figure 5.7, for which the substrate had been ion milled, the MCM-41 peaks at 3.84° and 4.33 °2-theta, corresponding to the (110) and (200) planes respectively, have relative intensities that are reversed from those of typical MCM-41 bulk samples. That is, the (200) reflection is more intense than the (110) reflection. This result appeared to be consistent for all samples from this batch. Figure 5.8 highlights the comparison by overlaying the spectra from both samples, as they are shown in Figures 5.4 and 5.7. This suggests that ion milling, resulting in differing surface energies associated with vertical and horizontal surfaces, has affected film structure, mesopore orientation, or both.

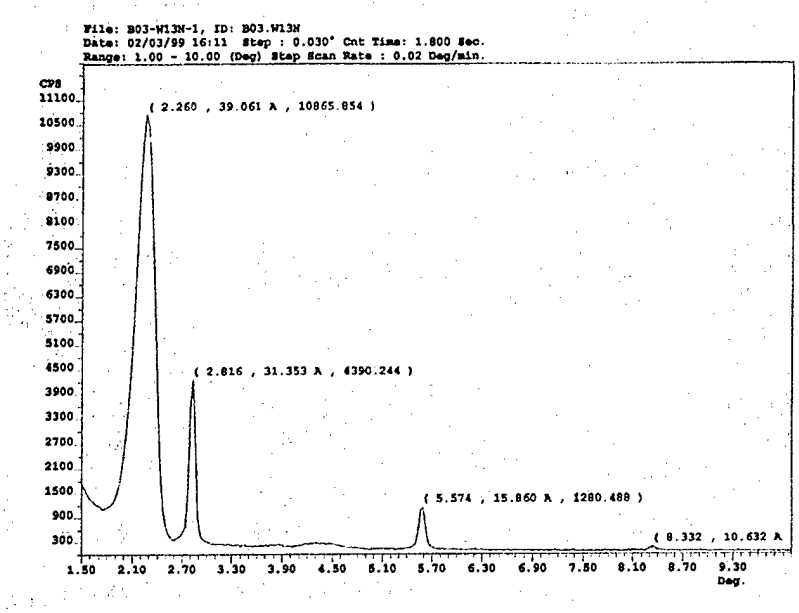

Figure 5.6: X-ray diffraction spectrum from a mesoporous silica film sample, obtained prior to calcination. Substrate was ion milled. Sample B03.w13n.

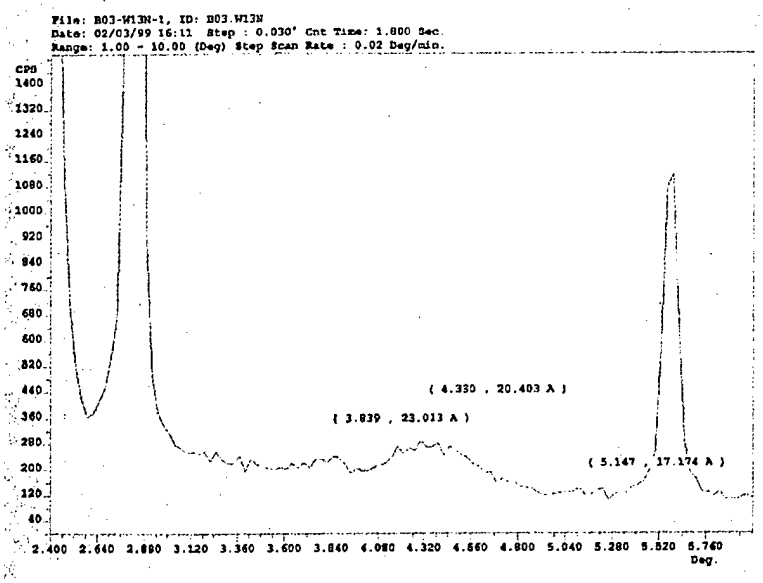

Figure 5.7: Close-up of the range 2.4° to 6.0° 2-theta shown in Figure 5.6. Sample B03.w13n.

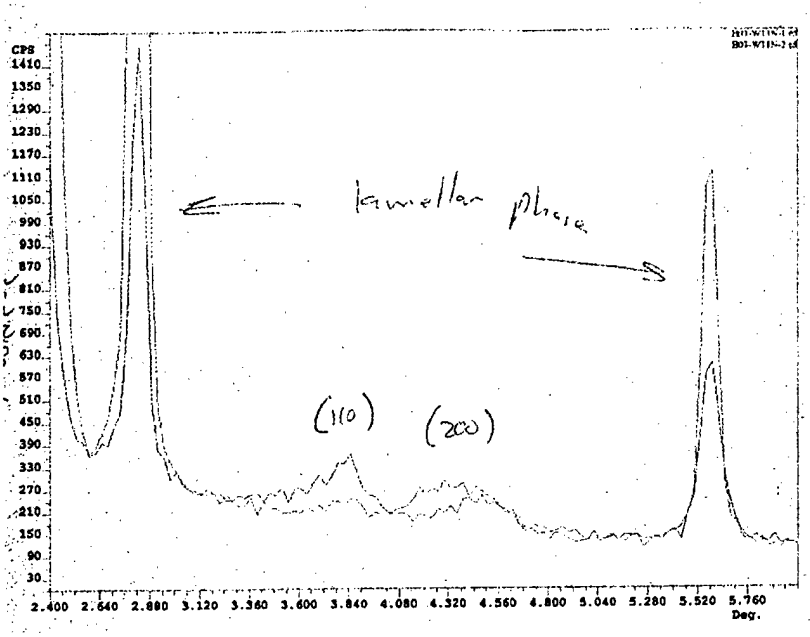

Figure 5.8: Overlay of Figures 5.4 and 5.7, highlighting the reversal in peak intensities of the (110) and (200) reflections. Samples B03.w11n and B03.w13n.

Mesoporous silica films were formed on Si/SiO_2 substrates by exposing the substrates to synthesis gels in closed containers held at various temperatures. Films were formed over varying time periods, following which the samples were removed from the gel to dry and cool. In early experiments, we held the gel at constant temperatures of either ~80° C or ~20° C throughout the film formation process, and all cooling occurred once the substrate was removed from the gel. Later, as described in the third section of Chapter Three, entitled "Preparation from Acidic Solution", the temperature at which films were formed was varied during growth, by cooling the gel in the presence of the substrate.

Film samples prepared in the early, constant temperature experiments were not stable to calcination. Figure 5.9 shows the x-ray diffraction spectra of a

mesoporous silica film sample prepared while holding the acidic synthesis gel temperature constant at room temperature for 30 days. The unusually long synthesis time was utilized to compensate for the slow rate of SiO_2 polymerization at room temperature. One spectrum was taken before calcination, the other after calcination at 150° C for four hours. Comparison of the two spectra shows that after calcination, the diffracted signal was much weaker, indicating a loss of order.

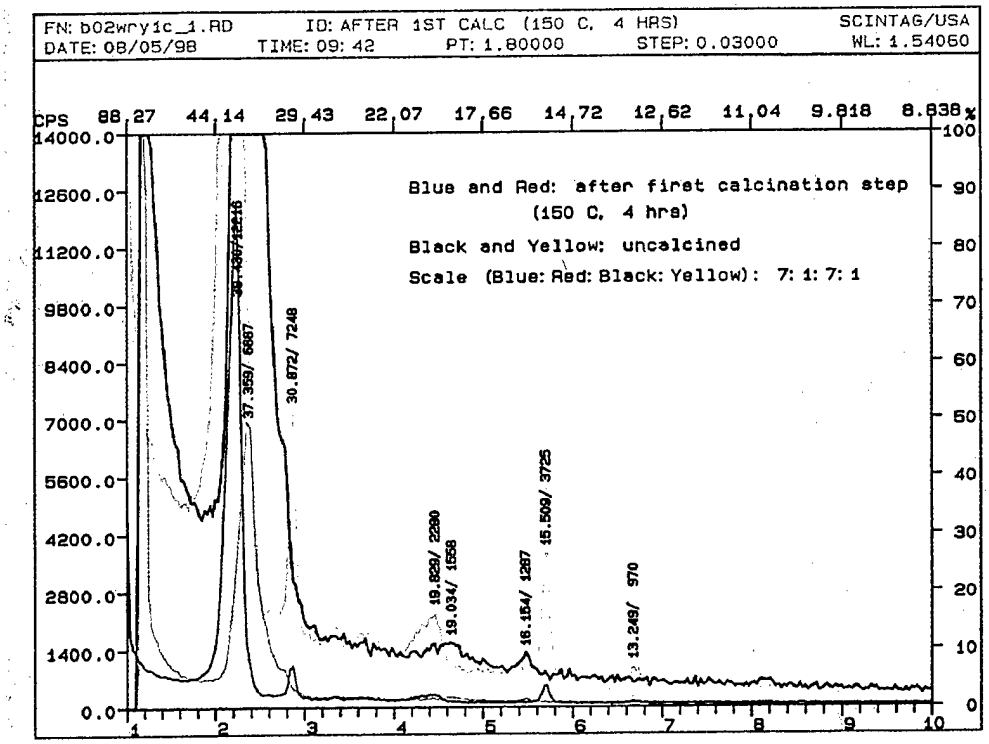

Figure 5.9: X-ray diffraction spectra from a mesoporous silica film sample prepared by acidic prep held at room temperature for 30 days. The spectra plotted in black and yellow were taken before calcination, and the spectra plotted in blue and red were taken after calcination at 150° C for four hours. Sample B02.wry1.

Figure 5.10 shows the x-ray diffraction spectrum for the same sample as is shown in Figure 5.9, this time after an additional calcination at 300° C. There is no longer evidence of any order at all; only background counts are observed. Samples from the same batch that were synthesized at ~80° C for from a few hours to a few days, rather than at ~20° C for 30 days, lost all order after calcining to only 150° C. These samples produced spectra similar to Figure 5.10. Compare these results with Figure 5.5, taken from a sample grown by the newer process of varying gel temperature in the presence of the substrate. Figure 5.5 shows that even after calcination at 650° C, samples from the newer process do not lose all evidence of order entirely.

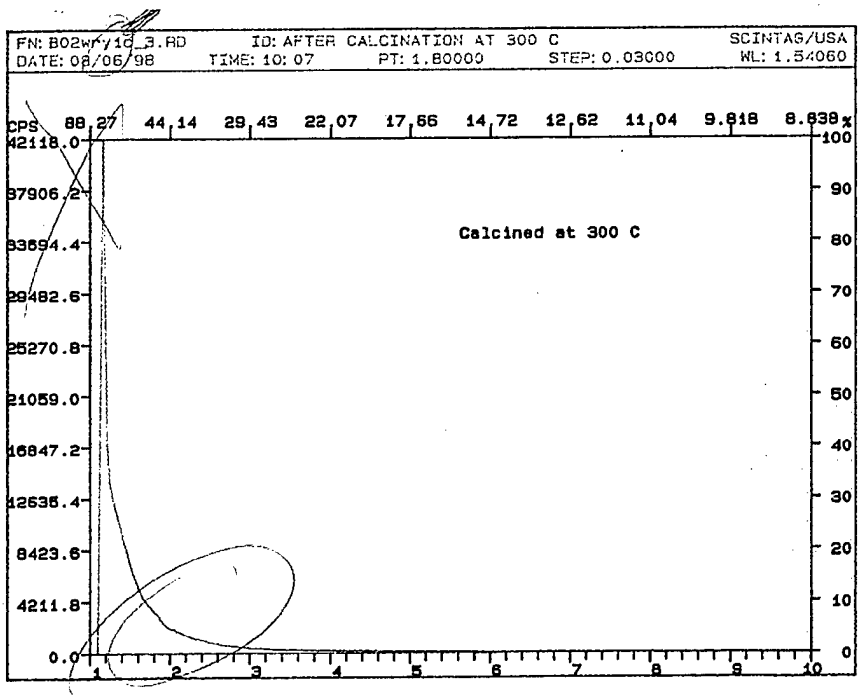

Figure 5.10: X-ray diffraction spectrum from the mesoporous silica film sample prepared by acidic prep held at constant temperature shown in Figure 5.9, after further heating to 300° C and subsequent cool-down. Sample B02.wry1.

Theta-Two Theta Measurements at Elevated Temperature

In order to determine just what changes films experience during calcination, and at just what temperatures these changes occur, high-temperature x-ray diffraction studies were conducted. In these studies, a hot stage enclosed in a chamber was mounted on the theta-two theta diffractometer. The sample was placed on a temperature-controlled holder inside the chamber. The studies were performed on samples previously prepared by the acidic synthesis process described in Chapter Three. The results from the most exhaustive high-temperature study are described below.

The temperature of the sample was ramped from 28° C to 650° C, at a rate of 1° C per minute (Note: the whole experiment took several hours. During this time, the temperature controller failed twice, and the sample returned to room temperature as a result. Each time, the sample was reheated as quickly as possible to the temperature at which the controller had failed.) Every 10° C (or more often), the temperature was held constant for about 9 minutes while a diffraction scan was run. Figure 5.11 shows several x-ray diffraction spectra of the sample at representative temperatures over the range of 30° C to 650° C.

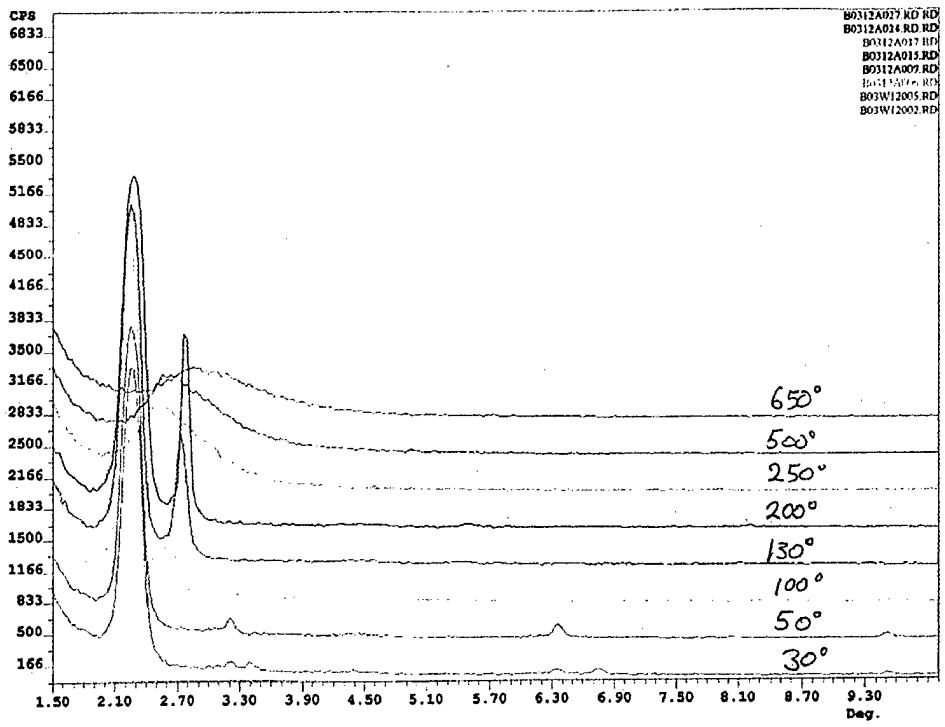

Figure 5.11: X-ray diffraction spectra taken at different temperatures of a mesoporous silica film sample that had been prepared by acidic synthesis. Sample B03.w12.

Similar to what was noted in the preceding section of this chapter, there is a potentially hexagonal phase in addition to two lamellar phases present in the sample in Figure 5.11. The primary peak at 2.25° 2-theta deteriorates above 200° C. Two significant phase changes occur in the lamellar phases, one between 40° and 50° C (see Figure 5.12), and the other between 96° and 100° C (see Figure 5.13). Figure 5.12 shows x-ray diffraction spectra for the sample at temperatures ranging from 28° to 50° C. From 28° to 40° C, there are two lamellar phases present. One of these disappears between 40° and 50° C.

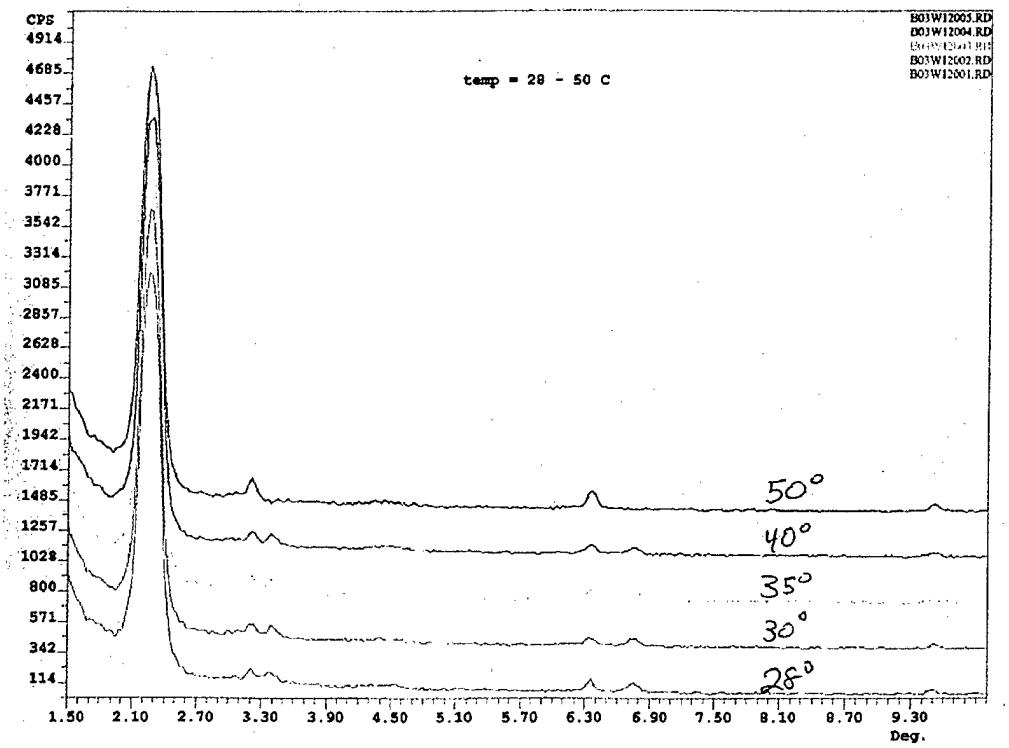

Figure 5.12: X-ray diffraction spectra of the same sample as shown in Figure 5.11, with detailed temperatures from 28° to 50° C. One lamellar phase disappears between 40° and 50° C. Sample B03.w12.

Figure 5.13 shows x-ray diffraction spectra for the sample at temperatures ranging from 90° to 100° C. A new peak appears at 2.62° 2-theta between 96° and 100° C, corresponding to a new lamellar phase. This phase becomes more and more pronounced as the temperature is ramped up from 100° C to 200° C, as can be seen from Figure 5.11.

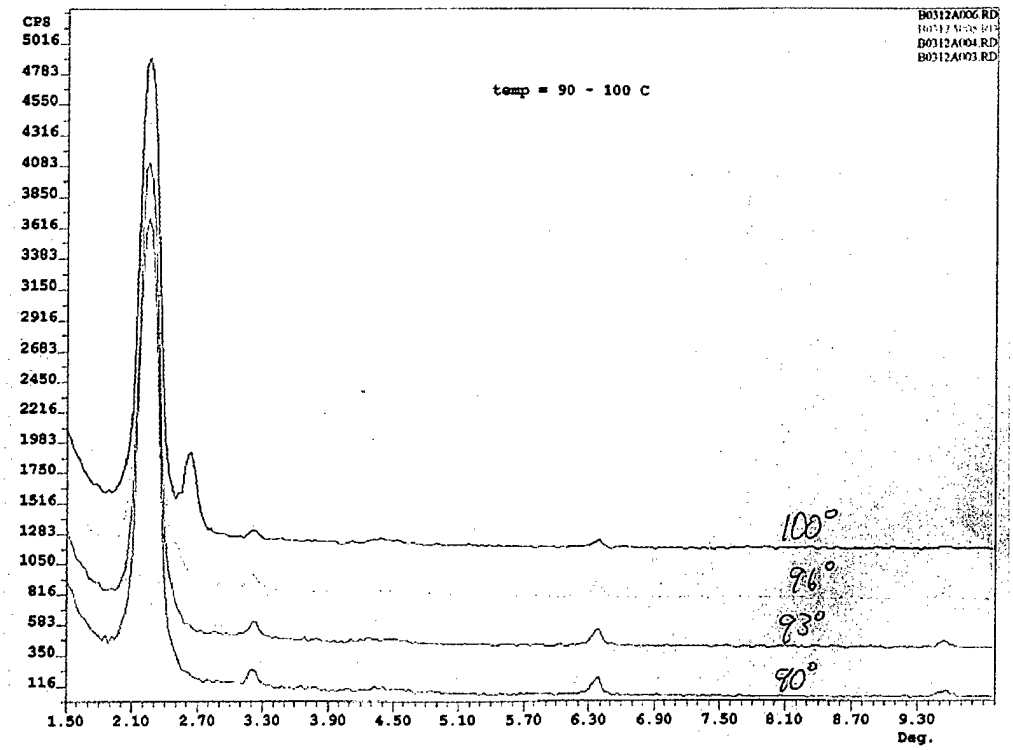

Figure 5.13: X-ray diffraction spectra of the same sample as shown in Figures 5.11 and 5.12, with detailed temperatures from 90° to 100° C. Sample B03.w12.

To better understand the behavior of mesoporous silica films at elevated temperatures, another high temperature x-ray diffraction study was done for comparison, this time on a film consisting only of surfactant (with no silica) on an Si/SiO_2 substrate. This sample was prepared as described in the third section of Chapter Three, entitled "Preparation from Acidic Solution", with three exceptions: (1) The silica source, TEOS, was not added to the reaction vessel.

(2) The mixture was held at room temperature, because at elevated temperatures micellar order is lost in the liquid phase.

(3) A substrate was dipped into the mixture for 20 seconds, and then removed and placed in a petri dish to dry naturally at room temperature.

The high-temperature x-ray diffraction study was then performed on the dried surfactant film. A number of phase changes were observed in the surfactant film as the temperature was increased from 30° to 230° C. Figures 5.14 through 5.18 show this evolution of diffraction spectra for the surfactant film. The temperature of the sample was ramped from 28° C to 360° C, at a rate of 1° C per minute. Every 10° C (or more often), the temperature was held constant for about 9 minutes while a diffraction scan was run. By the time the sample had reached 230° C, all evidence of order was gone (see Figure 5.18).

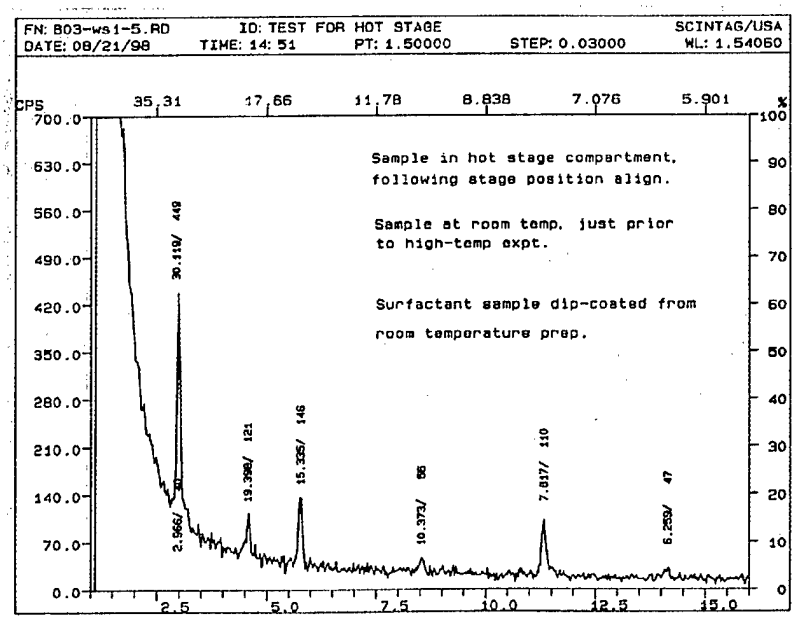

Figure 5.14: X-ray diffraction spectrum of surfactant film taken at room temperature just prior to temperature ramp up. Sample B03.ws1.

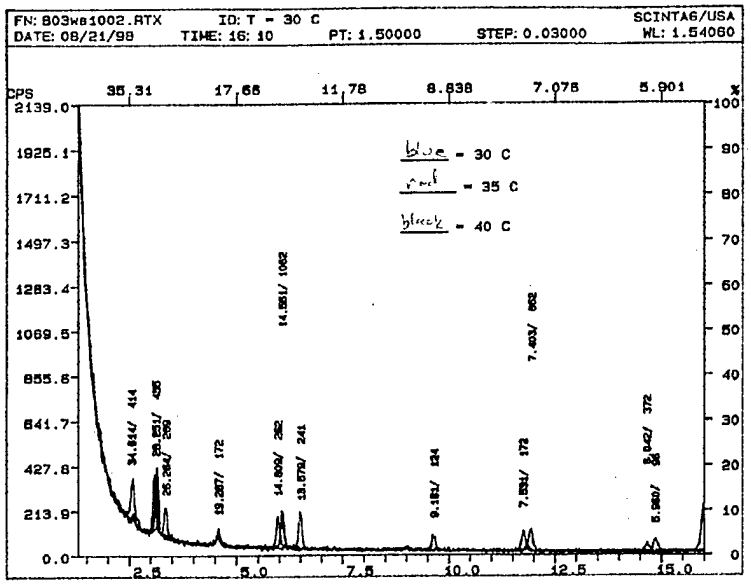

Figure 5.15: X-ray diffraction spectra of surfactant film for temperatures 30°, 35°, and 40° C. A phase change has occurred between 35° and 40° C. Sample B03.ws1.

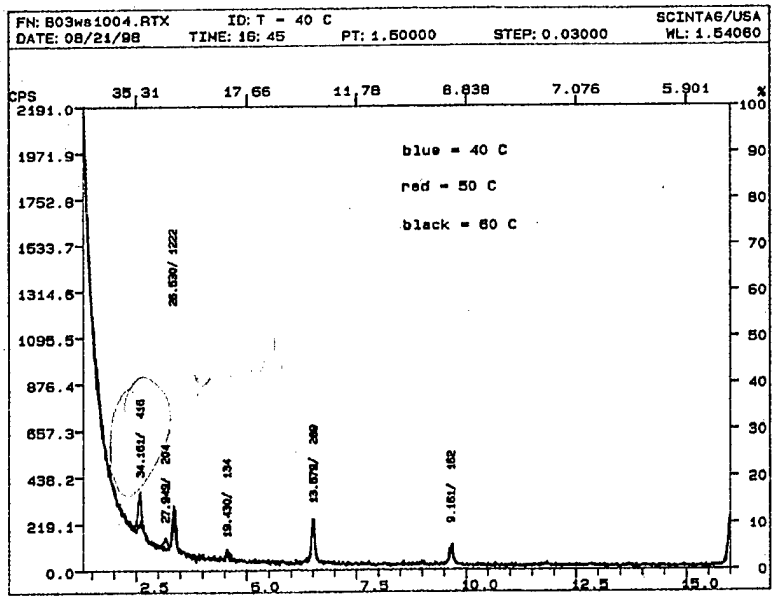

Figure 5.16: X-ray diffraction spectra of surfactant film for temperatures 40°, 50°, and 60° C. A phase change has occurred between 40° and 50° C. Sample B03.ws1.

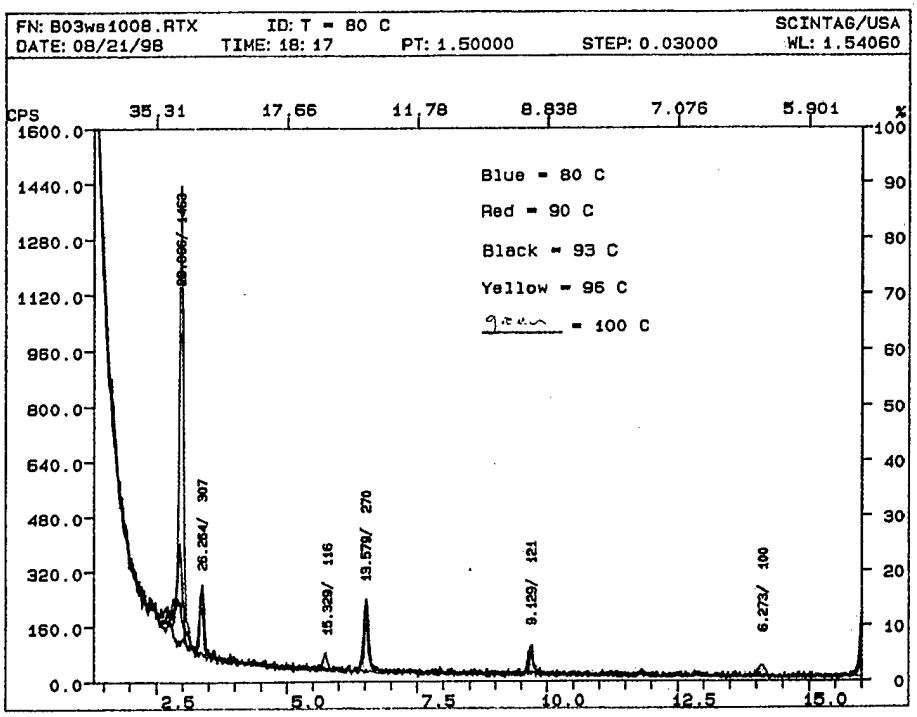

Figure 5.17: X-ray diffraction spectra of surfactant film for temperatures 80°, 90°, 93°, 96°, and 100° C. A phase change has occurred between 80° and 90° C. The peak with d-spacing = 30.0 Å grows dramatically in intensity from 90° to 100° C. Sample B03.ws1.

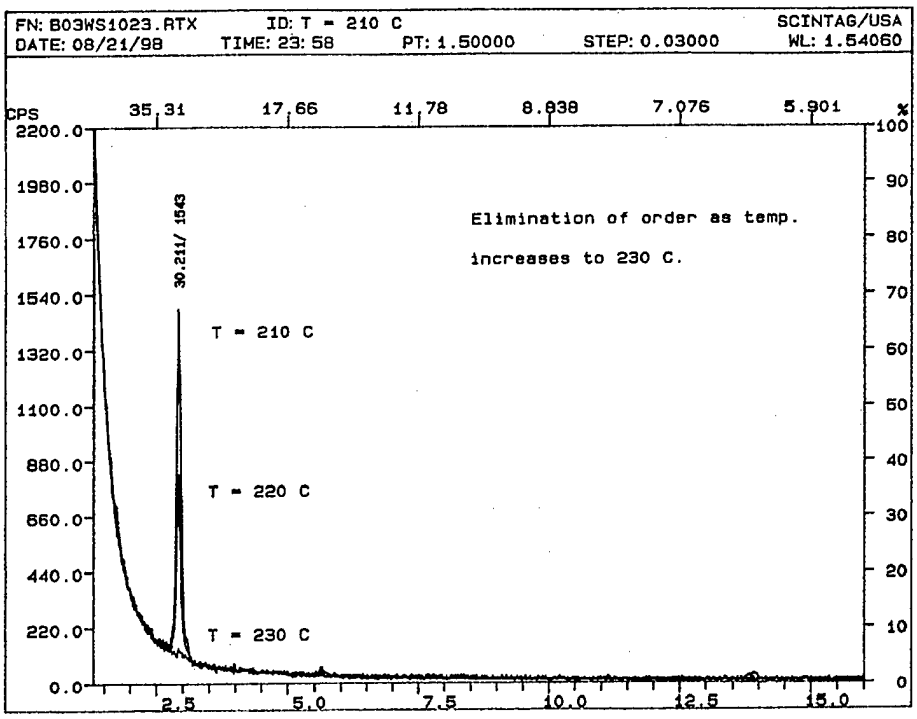

Figure 5.18: X-ray diffraction spectra of surfactant film for temperatures 210°, 220°, and 230° C. The peak with d-spacing = 30.2 Å decreases in intensity from 210° to 230° C, where it is no longer evident. This is the same peak that is shown in Figure 5.17 at 30.0 Å. The apparent difference in d-spacing was caused by the method used to determine peak position. Sample B03.ws1.

Reflection Pole Figures

The orientation of mesopores in mesoporous silica films on Si/SiO_2 substrates was investigated using x-ray diffraction pole figures in reflection geometry. Figure 5.19 shows the experimental setup for reflection pole figures.

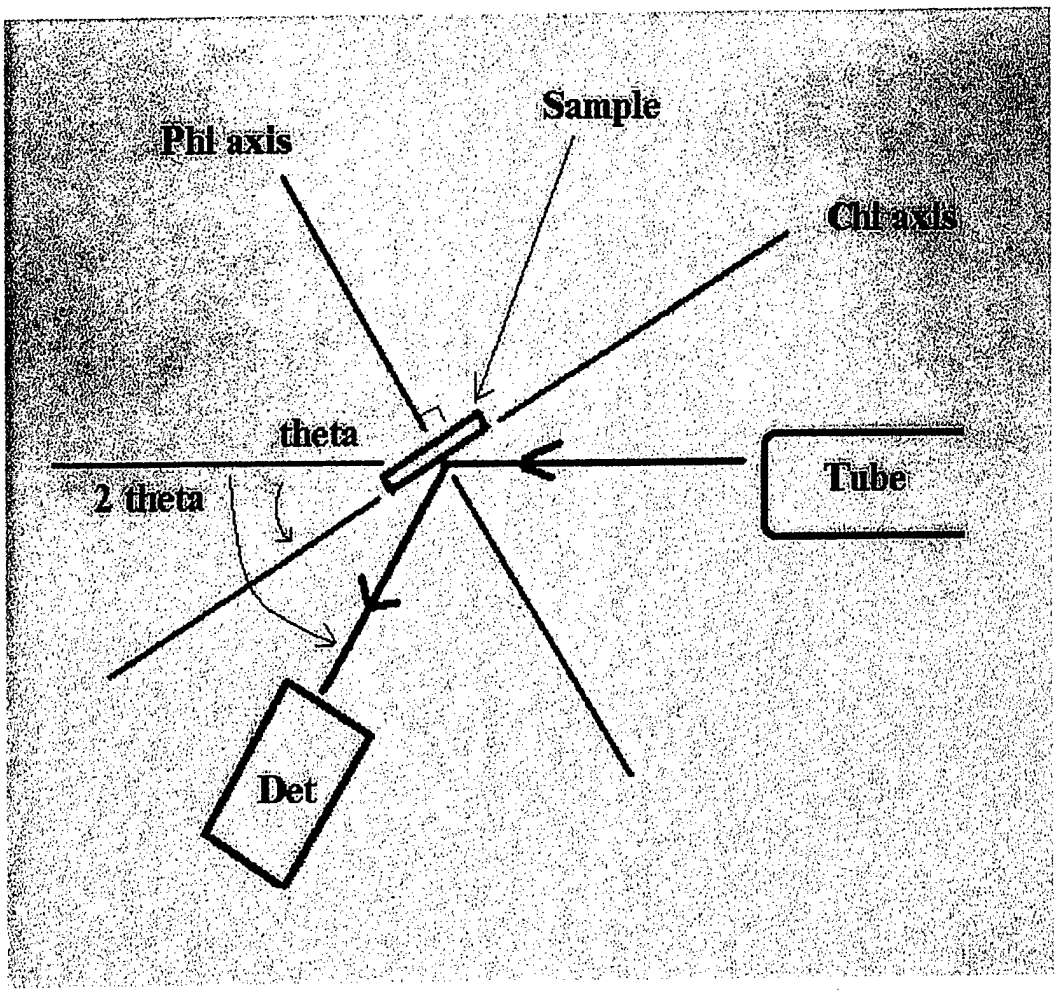

Figure 5.19: Experimental setup for x-ray diffraction pole figures in reflection geometry.

X-ray diffraction pole figures were obtained as follows. The detector and sample were aligned to the 2-theta and theta positions corresponding to the family of planes whose orientation was to be determined, in this case the (100) planes. These angles were held constant throughout the experiment. The phi-axis was set to zero, and the corresponding orientation of the sample with respect to this axis

noted. The chi-axis was set so that the surface normal of the sample was coplanar with the plane formed by the incident and diffracted beams (if these beams are idealized as rays). This corresponded to chi = 270° on the particular diffractometer utilized in the experiments described in this section. The shutter was opened, and phi was rotated through 360°, while collecting data every 5°. The chi-axis was then rotated 5° (which corresponds to tilting the sample), and the azimuthal scan about the phi axis was repeated. Similar azimuthal scans were done for increasing values of chi, until the chi axis had been rotated 80° in increments of 5° from its original position.

The pole figure analysis was used in an attempt to determine the orientation in 3-dimensional space, with respect to the substrate surface, of the (100) family of planes of mesopores in the film samples. For reference, Figure 5.20 shows the pole figure of a sample of bulk MCM-41 powder, in which the (100) planes are randomly oriented, as indicated by the wide distribution of reflections, and the minimal gradient in their intensities. In Figure 5.20 and subsequent pole figures (Figures 5.21 to 5.24), the scales indicate relative signal intensities. The centers of the plots are the origins of the phi-axes, and correspond to 0° of sample tilt (chi = 270°). The perimeters correspond to 90° of sample tilt (chi = 360°).

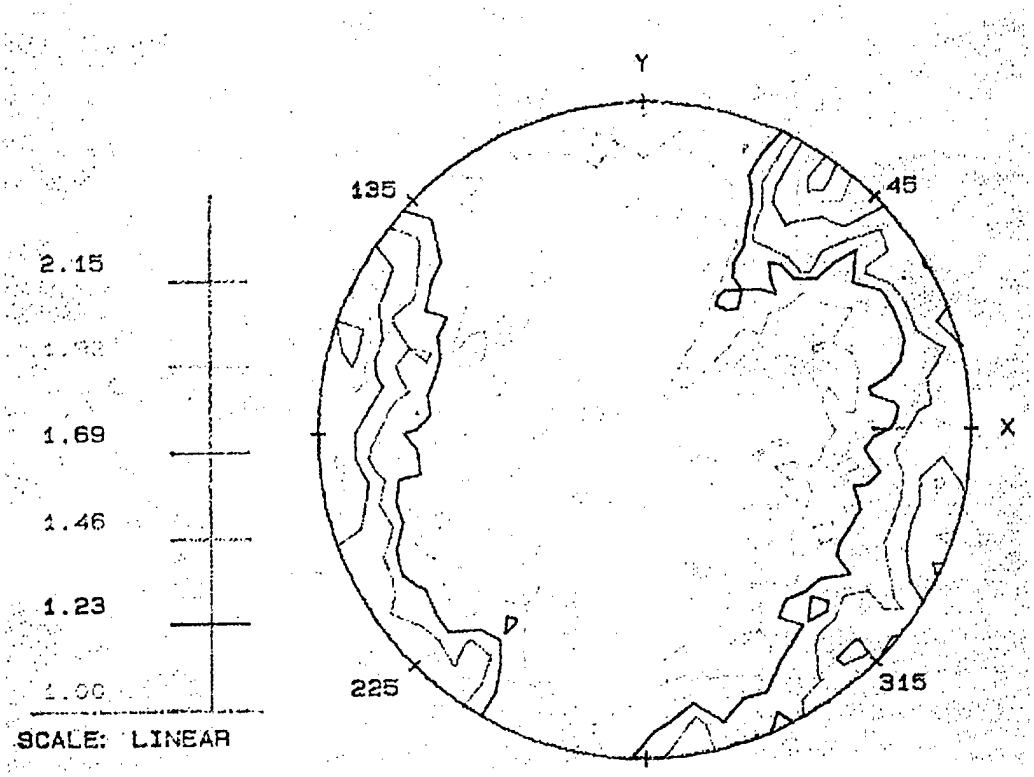

Figure 5.20: X-ray diffraction pole figure (reflection geometry) of a sample of bulk MCM-41 powder, in which the (100) planes are randomly oriented. The scale indicates relative signal intensity. The center of the plot is the origin of the phi-axis, and corresponds to 0° of sample tilt. The perimeter corresponds to 90° of sample tilt. Sample A05.b5n. Pole figure taken by N. Donnelly.

Obtaining accurate pole figures of mesoporous silica films on Si/SiO_2 substrates has proven to be problematic. Figures 5.21 and 5.22 show pole figures of a mesoporous silica film sample prepared by acidic synthesis as described in Chapter Three. Ordinarily, the high concentration of reflections at the center of these plots would indicate that the (100) planes in the film lie predominantly parallel to the horizontal substrate surface. In addition, there appears to be a

preferential orientation within the plane, as can be seen from the two lobes that appear 180° apart (in Figures 5.21 and 5.22, at phi = 90° and 270°).

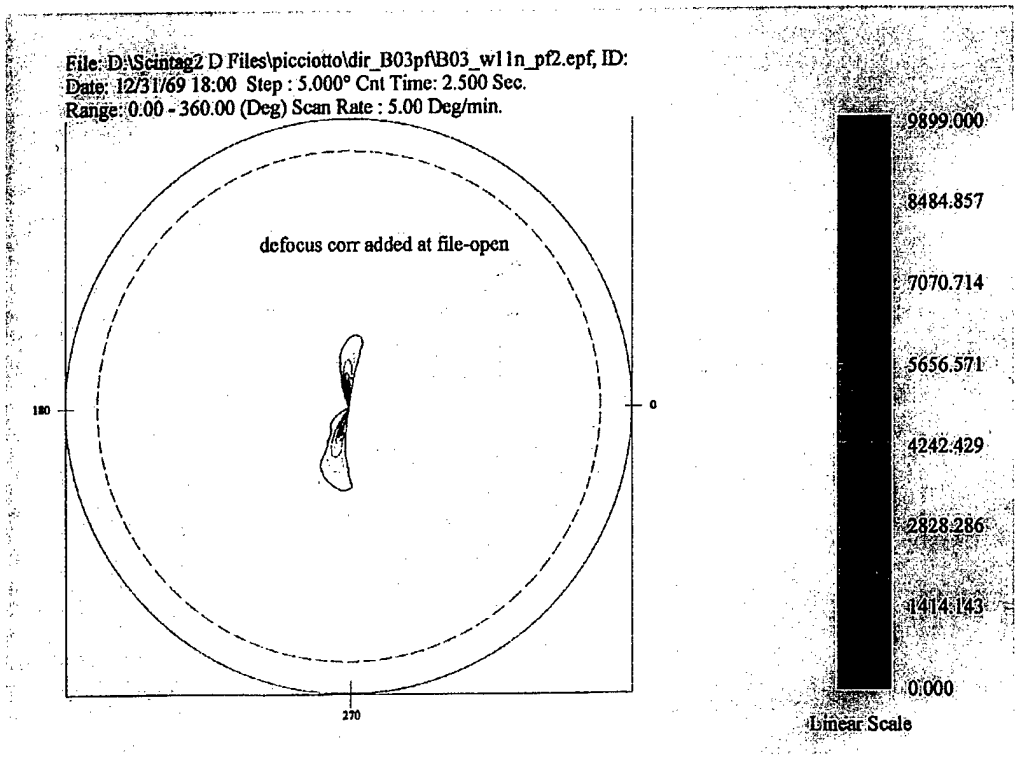

Figure 5.21: X-ray diffraction pole figure (reflection geometry) of an uncalcined mesoporous silica film grown on an Si/SiO_2 substrate. Poor alignment of the front surface of the sample with respect to the incident beam was responsible for the apparent orientation. Sample B03.w11n. (2/10/99 align)

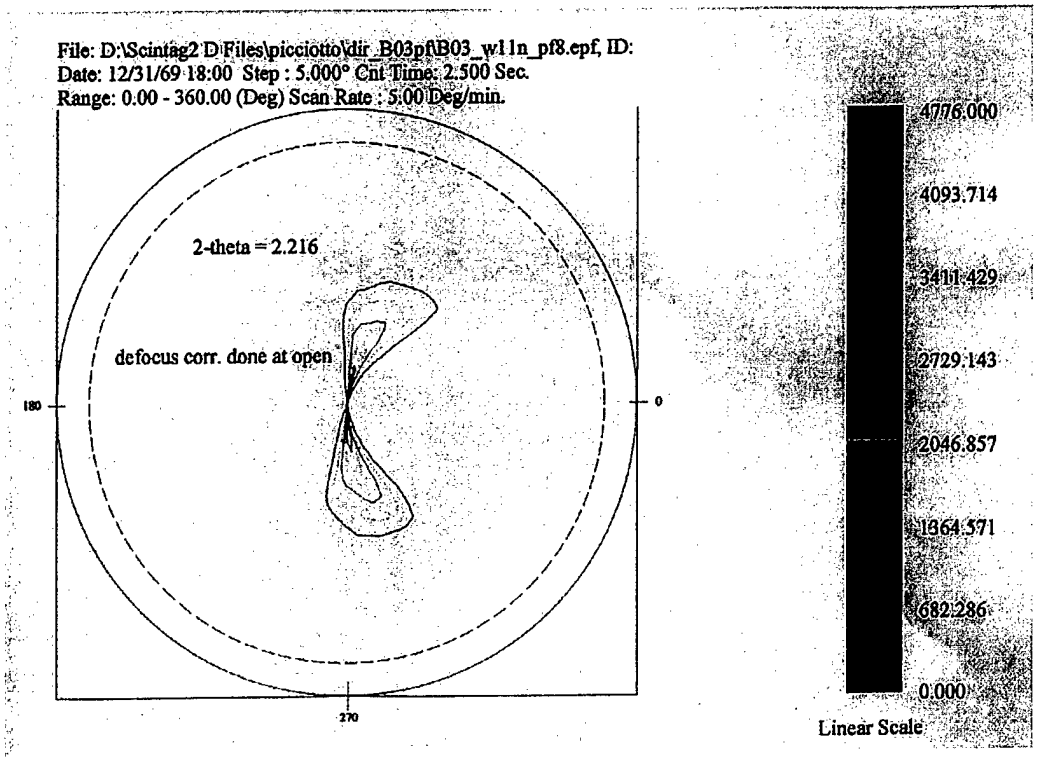

Figure 5.22: X-ray diffraction pole figure (reflection geometry) of an uncalcined mesoporous silica film grown on an Si/SiO_2 substrate. Poor alignment of the front surface of the sample with respect to the incident beam was responsible for the apparent orientation. Sample B03.w11n. (2/11/99 align)

Unfortunately, both the apparent orientation parallel to the substrate and the apparent orientation within these planes were actually due to an inability to align the pole figure diffractometer with sufficient precision. The large d-spacings (~40 Å) in these films required the x-ray beam to contact the samples at incident angles theta of ~1.1° with respect to the film surface. This small angle made the proper alignment of the front surface of the sample, the position of the detector, and the position of the collimator from which the beam emerged extremely critical.

It was possible, by taking considerable care in the alignment of the front surface of the samples, to obtain pole figures showing more nearly azimuthal symmetry. Figures 5.23 and 5.24 show such pole figures. Figure 5.23 was taken from the same sample as Figures 5.21 and 5.22, while Figure 5.24 was taken from another sample similarly prepared. The lobes that persist at phi = 45°, 135°, 225°, and 315° are artifacts. They arose because the samples were square in shape, with sides about 3 times larger than the diameter of the incident beam. Because the beam was narrower than the sample, and the incident angle theta was so small (~1.1°), when the beam was incident on either of the sample's diagonals it interacted with a sample volume greater by a factor proportional to $\sqrt{2}$, resulting in an increase in signal by a similar factor. Accordingly, within the precision allowed by the experimental setup, and contradicting the results shown in Figures 5.21 and 5.22, no azimuthal asymmetry was detected.

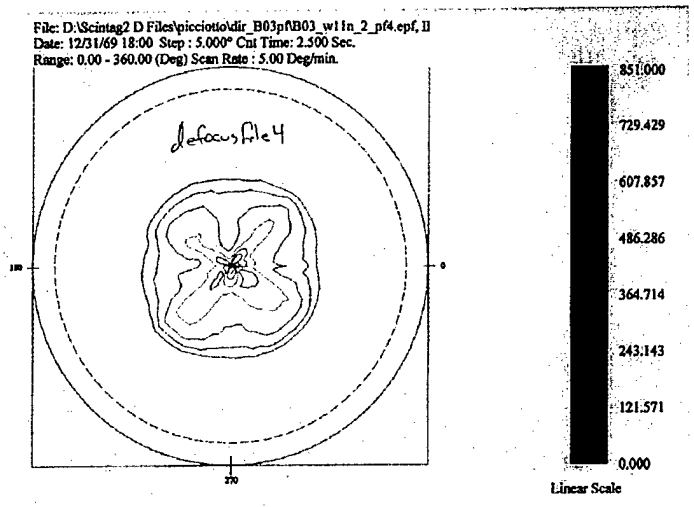

Figure 5.23: X-ray diffraction pole figure (reflection geometry) of an uncalcined mesoporous silica film grown on an Si/SiO_2 substrate. Compare Figures 5.21 and 5.22. Sample B03.w11n. (2/17/99 align)

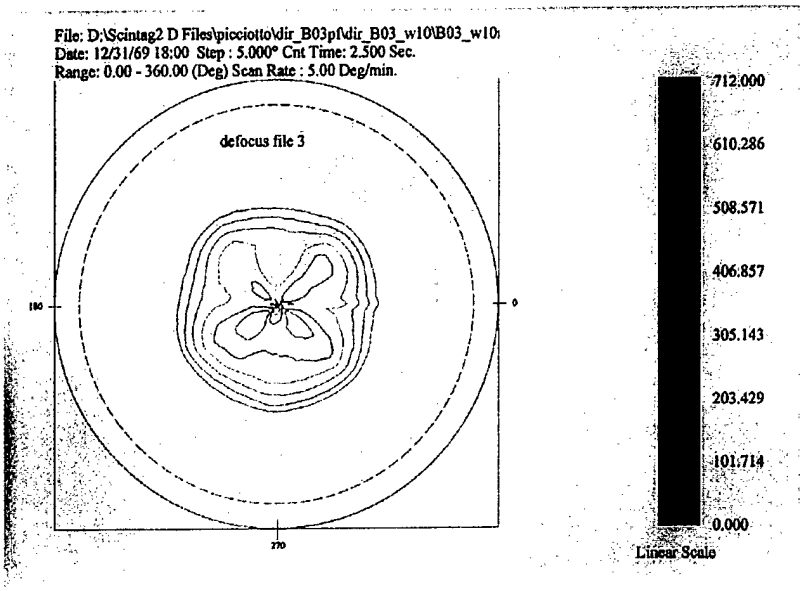

Figure 5.24: X-ray diffraction pole figure (reflection geometry) of an uncalcined mesoporous silica film grown on an Si/SiO_2 substrate. Sample B03.w10n. (2/25,26/99 align).

To further resolve the front surface alignment problem, silicon wafers for use as substrates with guaranteed miscuts of only +/- 0.1° were obtained from Virginia Semiconductor. It was hoped that these substrates would allow improved surface alignment in the reflecting geometry of the pole figure machine. However, it turned out that problems with the sample holder, variations in film thickness, and other alignment issues swamped the positive effect of truer substrates. These issues will be discussed further in Chapter Six.

Figures 5.23 and 5.24 appear to show high concentrations of planes of mesopores roughly parallel to (within 20° of) the substrate surface, similar to what is observed in Figures 5.21 and 5.22. However, this is actually an artifact of poor

collimator/sample alignment (and will be discussed in Chapter Six). Consequently, reflection pole figure experiments have provided no reliable evidence for any preferential orientation whatsoever of mesopores within mesoporous silica film samples. There was no reliable evidence that mesopore alignment in films differed from the random alignment of mesopores in bulk powder samples.

CHAPTER SIX: DISCUSSION OF RESULTS

High quality MCM-41 was prepared in bulk form by basic synthesis. Hexagonal ordering and uniform mesopore diameter were confirmed by TEM and x-ray diffraction, as reported in Chapters Four and Five. However, basic syntheses always resulted in the production of MCM-41 in particulate form. Typical particle dimensions were of the order of 1 micron. Individual particles contain large numbers of hexagonally ordered mesopores, but there is no alignment of mesopores from one particle to the next. If substrates are present in the reaction vessel, these MCM-41 particles may precipitate onto them, but actual growth of MCM-41 films at the substrate/liquid interface was not observed. This was confirmed by SEM, and can be seen from the examples presented in Chapter Four (Figures 4.5 and 4.6). In order to produce MCM-41 films grown at the substrate/liquid interface, with pore orientation over length scales of microns and greater, it was necessary to work with acidic syntheses.

Ordered films were successfully fabricated on Si/SiO_2 substrates from acidic synthesis preparations, which demonstrate the presence of some hexagonal ordering as determined by x-ray diffraction. However, these films also had other phase(s) present, most notably a well defined lamellar phase, that possibly consisted only of surfactant rather than templated silica. The AFM and TEM results of these mesoporous silica films, presented in Chapter Four, suggest that the pores were poorly ordered. However, the AFM results are difficult to interpret and the images were obtained under difficult conditions, owing to the very rough surfaces of the samples. Due to the quality of the samples produced to date, AFM does not appear to be an effective characterization technique for these materials at the present time.

SEM results confirmed that while acidic syntheses did produce some particulate MCM-41 (see Figures 4.7 and 4.8), films were also being formed on the substrates. Figures 4.9 to 4.13 all show films produced on Si/SiO_2 substrates during acidic syntheses. These films were generally not very uniform in appearance (see Figures 4.9 and 4.13), and were often discontinuous. The films typically cracked upon drying. Figures 4.10 and 4.11 show a film that has cracked into domains of about 50 microns to 150 microns in size.

SEM was useful in revealing macroscopic properties of mesoporous silica particles and films. However, even with a field emission SEM, it was not possible to resolve features on length scales of 25 Å, hence it was not possible to image individual mesopores by this technique. Since the requisite resolution was unobtainable by SEM, and inconclusive with AFM, characterization efforts needed to focus on x-ray diffraction and TEM.

TEM specimen preparation of bulk mesoporous silica samples was straightforward (see Chapter Four). However, difficulties were encountered in preparing TEM specimens from films. The polishing process sometimes resulted in the film being removed from the substrate when the wax used to hold the sample in position was removed. This is attributable to a lack of continuity in the films, and to poor adhesion of the films to the Si/SiO_2 substrates. A few images of films were nevertheless obtained, however very few pores were observed, and these exhibited no hexagonal ordering (see Figures 4.3 and 4.4). Nevertheless, x-ray diffraction results for these films showed hints of hexagonal ordering. It is possible that the films were damaged during TEM specimen preparation, since some films didn't survive this process at all. It is also possible that a deficiency of TEOS (the silicate source) in the synthesis reaction led to poorly ordered materials. This is plausible because the presence of silicate dramatically alters the surfactant concentration

necessary in the reaction to achieve hexagonal ordering. A test film produced in reaction conditions with surfactant concentration equivalent to that in mesoporous silica acidic syntheses, but no silica source added, had lamellar x-ray diffraction spectra (see Figure 5.14). No evidence of hexagonal ordering was observed in the surfactant film at all.

Theta-two theta x-ray diffraction results revealed the presence of a high degree of hexagonal order in bulk materials synthesized in basic preparations (see Figures 5.1 and 5.2). Post-calcination (100) d-spacings were consistent with pore sizes observed by TEM (see Figures 5.2, 4.1 and 4.2). Similar diffraction studies performed on films synthesized in acidic preparations indicated that there was some hexagonal ordering, but that additional unwanted lamellar phases were also present (see Figures 5.3, 5.4, 5.6, and 5.7).

Theta-two theta diffraction also revealed differences in film samples grown on ion-milled vs. uniformly fluoropolymer-covered substrates (see Figure 5.8). The differences in relative (110) and (200) peak intensities suggest that surface energy modifications did indeed affect film growth. However, it is not known whether the observed differences in the x-ray diffraction results are due to structural differences in the film, orientational differences of the mesopores within the film, or both. It is likely, though, that the vertical surfaces (trench walls) on the substrates did not play a measurable role, and that the measured effect is due solely to surface energy differences. This is because greater than 90 % of the substrate's surface area available for film growth was horizontal. Four possible explanations suggest themselves.

The first possible explanation is that the fraction of material in the lamellar phase vs. that in the hexagonal phase is simply greater in the ion-milled samples, where $I_{(200)} > I_{(110)}$ ($I_{(hkl)}$ is the intensity of the reflections from the (hkl) planes).

This is plausible since there would be no (110) reflections from a lamellar sample. This explanation is attractive owing to its simplicity.

A second possible explanation is that there is a higher fraction of mesopores parallel to the substrate's horizontal surface in the ion-milled samples. For the experimental setup used, (110) reflections would be absent from the diffraction spectrum of perfectly horizontal mesopores. This has been found to be the case by other groups who report horizontal mesopores and no (110) reflections at all. This second explanation assumes that in general, the mesopores are distributed in a variety of orientations within the film. Such an assumption seems consistent with the pole figure evidence reported in this thesis.

A third possible explanation is that the SiO_2 walls between the mesopores may be incompletely formed. This explanation was suggested by K. Edler, following the results of a group of researchers who modeled x-ray diffraction spectra as a function of time during mesoporous silicate formation, and found that incomplete walls, or walls with holes in them, should lead to $I_{(200)} > I_{(110)}$. However, it is not obvious that the presence or absence of fluoropolymer on the surface of the substrate would affect the rate of silicate condensation in the walls between mesopores, leading to varying degrees of wall formation between samples.

The fourth, and most improbable possible explanation, is that the fluoropolymer monolayer in the non-ion-milled samples reacted chemically with the mesoporous silica synthesis gel during film formation, resulting in some sort of structural difference in the film. While this may well have occurred, it is unlikely that any effect would have been measured in x-ray diffraction experiments, since the quantity of fluoropolymer available to react was very small.

The studies reported in this thesis do not contain sufficient data to allow a decision to be made concerning which of these four explanations is correct.

Nevertheless, the author believes that the third and fourth explanations given above are the least likely.

Multiple Phases and Phase Changes in Mesoporous Silica Films Observed by Temperature-Dependent Theta-Two Theta X-ray Diffraction

In order to learn more about the multiple phases, and to more carefully study the stability of the films to calcination, temperature-dependent x-ray diffraction studies were performed. The discussion in this section concerns the results reported in Chapter Five in the section entitled "Theta-Two Theta Measurements at Elevated Temperatures".

Films grown in synthesis conditions where the growth temperature varied during the growth process withstood subsequent elevated temperatures much better than films grown at constant temperatures. X-ray diffraction results from film samples grown at constant temperatures of ~20° C showed that these films were unstable to elevated temperatures as low as 150° C held for 4 hours (see Figure 5.9). All mesoscopic structure was lost following heating to 300° C (see Figure 5.10). In contrast, films grown by the process outlined in Chapter Three in the section entitled "Preparation from Acidic Solution" withstood temperatures up to 200° C for several hours without loss of structural order (see Figure 5.11). These films withstood further heating to 650° C without losing evidence of structure entirely (see Figure 5.11).

Both types of films discussed above contained a hexagonal, MCM-41-like phase as desired. The quality of the hexagonal phase was improved in the more stable, later films. The films also contained other phase(s), which looked lamellar. These lamellar phases may have been templated silica, or they may have consisted of surfactant only. The presence of surfactant was expected, since the films had not

yet been calcined to remove the surfactant template from the pores. If the lamellar phase consisted of surfactant only, this may mean that the synthesis gels were surfactant-rich, or, viewed another way, that there was a deficiency of silica source (in this case TEOS) in the gel. This would be consistent with the suggestion of M. Lim that the absence of strong hexagonal ordering as evidenced by both TEM and x-ray diffraction was due to a deficiency of TEOS in the reaction gel.

There are two indications that the lamellar phase in the films is not mesoporous silica but consists of surfactant only. In comparing Figures 5.11 and 5.18 at temperatures near 200° C, it is observed that both samples exhibit loss/reduction of order at the same temperature, and both have roughly the same d-spacing of ~30Å. A larger d-spacing would be expected in the lamellar phase of the silicate sample if this lamellar phase contained silicate, since the silica would occupy a finite volume between the surfactant template layers.

Determination of Mesopore Orientation Using X-ray Diffraction Pole Figures

Pole figure analyses were used in an attempt to determine the orientation of specific "crystal" planes in mesoporous silica film samples. It is important to note that this technique does not provide information about crystal structure (in the present case, lamellar vs. cubic vs. hexagonal). It is therefore important to be clear on the structure of the sample for which pole figure data is taken. One could have a lamellar film oriented parallel to the substrate, and the pole figure would be identical with that of a hexagonal film oriented parallel to the substrate. Structure information was obtained by theta-two theta geometry x-ray diffraction, as discussed previously.

The results obtained by doing pole figures in reflection geometry initially suggested (Figures 5.21, 5.22) that the mesopores in the examined films were

oriented primarily parallel to the substrate's horizontal surface. The results further implied that there was alignment within this substrate plane along some directing axis, i.e. that there was some azimuthal or phi dependence. It was therefore tempting to conclude that the substrate surface had influenced the alignment of the pores in some way, and that we could hope to exploit this property by the strategy of preparing vertical surfaces on the substrates, as discussed in Chapter Three in the section entitled "Substrates". However, the concern was raised by D. Ast that some spurious geometric effect, rather than alignment in the film, might be responsible for the appearance of the results. One clue that the observed azimuthal assymetries were artifacts is that both Figure 5.21 and Figure 5.22 are pole figures of the same sample, taken one day apart (with realignment done in between). The two plots look like mirror images of each other. Possible problems with the experimental setup were investigated, leading finally to the following conclusions.

First it was found that the front surface of the samples were not mounted sufficiently "flat" (i.e., normal to the phi axis, see Figure 5.19). This alignment is crucial owing to the very small incident angle theta at which the x-ray beam encounters the sample. When poorly aligned, the edge of the substrate can block the beam from hitting the film for a certain range of angles. The beam attenuates in the substrate, and no signal is observed at the detector. When the sample has rotated azimuthally (about the phi axis) to 180° from these angles, the beam has to pass through the substrate after encountering the film and before striking the detector, which again results in attenuation and no observed signal. This situation is consistent with the azimuthal (phi) assymetries observed in Figures 5.21 and 5.22.

Further difficulties in front surface alignment of the sample in the diffractometer were found to arise from the film surface being uneven and rough,

and the film thickness varying considerably throughout the sample. This means that the position of the surface is effectively ill-defined.

D. Ast suggested using low miscut substrates to simplify alignment procedures. It had been determined that the substrates used, which were test-grade Si (100), had surfaces that were miscut with respect to the (100) planes by 1° or more. Si (100) substrates were ordered from Virginia Semiconductor with guaranteed miscuts of no more than +/- 0.1° with respect to the (100) planes. However, any benefit derived from using these substrates was overwhelmed by the other alignment issues discussed below.

After careful attempts to improve upon front surface alignment, that included the use of a laser, back reflection Laue camera, and other techniques, improvement was obtained in the pole figure results (see Figures 5.23, 5.24). These results effectively eliminated the conclusion that there was any alignment of mesopores within planes parallel to the substrate's horizontal surface. Further, they suggested that the pores were predominantly arranged at angles of ~20° to the substrate's horizontal surface, rather than being predominantly parallel, as the first results had indicated. However, this indication of alignment is also highly suspect, for the reasons outlined below.

It was not possible to align the collimator with sufficient precision such that the beam encountered the sample at the intersection of the phi and chi axes (see Figure 5.19). The problem is that the available adjustments on the diffractometer are too coarse. A related problem was the inability to align the sample front surface with sufficient precision such that it was placed at the intersection of the phi and chi axes. These two misalignments cause the sample to move into and out of the beam as the sample is tilted (rotated about the chi axis) during the experiment. As the sample moves in and out of the beam, the diffracted beam intensity varies

significantly. The sample was found to be able to move entirely out of the beam during the experiment, leading to a diffracted beam intensity of zero. The consequence is diffracted signal intensity that is a strongly varying function of tilt (value of chi) due to systematic error. Since the purpose of the experiment is to determine the orientation of pores with respect to the substrate surface (vertical, horizontal, or in between) by examining diffracted signal intensity as a function of tilt (value of chi), these misalignments pose a fatal problem for the experiment.

Another issue with reflection pole figures that could not be properly addressed at all is the issue of defocus corrections. Defocus corrections are applied to pole figure raw data to correct for the fact that at increasing tilt (advancing values of chi) the diffracted signal intensity should decrease in a predictable, or at least measurable, way. This decrease arises from the reduced volume in the sample with which the x-ray beam is able to interact. Correction files are created by measuring the diffracted beam intensity as a function of chi for a randomly oriented test sample that is otherwise equivalent to the sample of interest. Since this test sample is randomly oriented, the diffracted beam intensity should not depend on chi. However, dependence will be observed owing to the reduced volume of interaction discussed above. The corresponding (false) dependence in real samples can then be corrected. This is done by multiplying the measured signal intensity at a given value of chi by a factor equal to the ratio of the test sample's measured intensity for chi equal to zero (no tilt) to the test sample's measured intensity at the given chi. Owing to the alignment problems discussed above, it was not possible to obtain meaningful defocus correction files for mesoporous silica film samples.

CHAPTER SEVEN: SUMMARY AND FUTURE WORK

Summary

High quality mesoporous silica possessing hexagonally ordered uniform diameter pores (MCM-41) was synthesized in particulate form from basic preparations. Ordered mesoporous silica films were grown from acidic preparations on oxidized patterned silicon substrates with various surface coatings. These films, while ordered, did not convincingly display hexagonal ordering, and possessed unwanted lamellar phases. The unwanted lamellar phases and minimal hexagonal ordering were probably due to a deficiency in the silica source (TEOS) in the synthesis reaction. The films were discontinuous, inhomogeneous, and very rough. No evidence was found to indicate that mesopores were preferentially ordered normal to the horizontal substrate surfaces. Neither was there any evidence found to indicate that mesopores were oriented with any preferential direction at all. However, x-ray diffraction results suggested that controlling the surface energy of the substrate surface affected either the mesoporous silica films' structure, its orientation, or both. The best films were able to withstand temperatures up to 200° C without loss of order, and up to 650° C without losing evidence of ordering completely.

TEM and x-ray diffraction were found to be the only reliable methods of characterization of samples at mesoscopic length scales. TEM specimen preparation of films was problematic and partially unsuccessful. Theta-two theta x-ray diffraction successfully yielded structural information for both particulate and film samples. X-ray diffraction pole figures in reflection geometry were unsuccessful in determining mesopore orientation within films, because the

available diffractometer could not be aligned with the precision necessary for the very small (~1.1°) incident angles required.

Future Work

Synthesis

A useful tactic may be to calcine films immediately after synthesis, in order to freeze in their structure. Left to dry naturally, films dry very slowly, and exhibit changes in x-ray diffraction spectra as time progresses (on a scale of days).

If more work is done using the acidic synthesis procedure outlined in Chapter Three, the TEOS concentration in the reaction should be increased significantly. Further stirring should also be done to better homogenize the reaction mixture.

The effect of varying growth temperature during film synthesis on final film quality should be further explored. For example, the surfactant-water-acid mixture could be heated to eliminate ordering prior to introducing either the substrates or the silicate source. The mixture could be cooled while adding these, or immediately prior to adding them. In any case, care should be taken with elevated temperatures because too high temperatures for too long a time can result in zeolite production, which is undesirable.

Ordering of the micellar template diminishes at elevated temperatures, but higher temperatures are needed to promote silicate condensation. To produce highly ordered films, it might be worth investigating chilling the reaction mixture to preserve micellar order and finding a chemical agent to facilitate silicate condensation at these lower temperatures. Condensation must nevertheless be slow enough so that it can occur on the surface of the substrate instead of rapidly throughout the entire solution.

Orientation

As a strategy for orienting mesopores normal to substrate surfaces, trenches with hydrophobic sidewalls is probably not optimal. An alternative approach might involve growing films on Si (111) surfaces, as these present a hexagonal arrangement of atoms, and some researchers[33,35,36] have reported results from which they have argued that substrate crystal structure can affect orientation of mesopores in films grown upon them. While these experiments were done with graphite, it may be worth trying with silicon.

Alignment might be enhanced by the presence of electric fields. Both DC and AC fields should be tried. Another approach would be to try micromolding in capillaries, following the process developed by Trau, et al.[47], but modified to utilize vertical capillaries.

Films generally adhered poorly to surfaces. This may be due to a surfactant layer or layers forming on the substrate surface prior to the initiation of film growth. This would not be unexpected behavior for surfactants[35], and a way to eliminate it will need to be found to enable use of the film as a template for germanium dots.

Characterization

Characterization of the mesoporous silica films continues to be a critical issue. Here, x-ray diffraction and TEM complement each other nicely. Both techniques can access the length scales necessary (~25Å) to observe mesopores. While TEM can provide direct micrographic evidence of mesopore existence, size, uniformity, ordering, and alignment with respect to a surface, it does so only over a very short length scale. X-ray diffraction, although an indirect measurement of the system, nevertheless averages over length scales several orders of magnitude larger

than the dimensions of regions imageable by TEM. Theta-two theta diffraction experiments can provide information about mesopore spacing and ordering. Pole figure experiments can provide information about alignment of mesopores with respect to surfaces.

For TEM to be effective, two things are needed. First, films need to be reasonably continuous, if they are freestanding or removed from substrates for imaging. Second, films that adhere reasonably well to substrates are needed to demonstrate mesopore orientation at the substrate-film interface. Ultramicrotomy should be explored as a method of preparing TEM specimens of both freestanding films and films adhered to substrates. The best demonstration of mesopore orientation will show what happens to the mesopores as they contact the substrate. Ultramicrotomy may be the only means to prepare the necessary TEM specimens.

Theta-two theta x-ray diffraction experiments continue to be a very fast way to check for structure and order in mesoporous silica samples. What is needed is to develop pole figure techniques that can provide reliable and accurate data on mesopore orientation. Both reflection and transmission experiments are needed in order to cover the full range of possible orientations of mesopores on substrate surfaces. Silicon substrates with x-ray transparent windows might be developed to facilitate transmission pole figure experiments, which are required in order to access the space that includes mesopores oriented normal and nearly normal to substrate surfaces.

Other Issues and Concerns

There are some additional considerations that should be addressed to ensure that mesoporous silica films on oxidized silicon substrates will be able to serve their intended purpose, that is, as a template for the patterning of ordered arrays of

germanium dots. One concern is the typical lattice contraction observed in mesoporous silicates upon calcination. This may result in discontinuities in the film, poor adhesion of the film to the substrates, or other difficulties. This lattice contraction can be reduced by modifying synthesis temperatures, but perhaps not without introducing other undesirable effects.

Another concern is that ideally, mesopore lengths (i.e. film thicknesses) should be as small as possible, for ease of germanium deposition through the pores. It is possible that the germanium will stick to the pore walls and clog them up, similar to what was reported in molecular beam epitaxy experiments by Tang, et al. at UCLA[48,49]. It is possible to coat the walls of the mesopores with various chemicals[50,51], and such a strategy may be needed to reduce germanium "sticking".

A third concern is the fact that neither end of the pores may actually be open. It seems likely, at least on the end of the pores at the top surface of the film, that the organic micelles would form domed "lids". This is plausible since otherwise the hydrophobic tails of surfactant molecules at the end of the micelle would be in contact with water. If the micelles are domed, silica will most likely cover them. It is not clear what the fate of the silicate lids would be during the calcination process. Calcination may solve this, if it is an issue at all, but calcination is unlikely to help if the substrate end of the pores is similarly capped.

Many researchers are actively engaged in developing low-k dielectrics for device and integrated circuit applications. Some researchers have expressed interest in mesoporous silica films as potentially very good candidates for this application, since they possess large volume fractions of air. This is worth exploring further, once mechanically stable high quality films are available.

APPENDIX A: Theta-Two Theta X-ray Diffraction of Mesoporous Silica Films (Procedural Notes)

These notes concern x-ray diffraction of large d-spacing (> 15 Å) films, either free-standing or on substrates. In their particulars, they apply to theta-two theta diffraction done on the "Scintag I" diffractometer in the CCMR X-ray Diffraction Facility managed by M. Weathers.

1) Sample Mounting: the top surface of the film must be positioned properly to avoid systematic error in measured Bragg angle leading to error in calculated d-spacing. The top of the film should be positioned at a height that is flush with the stops that arrest the motion of the spring-mounted sample stage. Accomplishing this may involve using pieces of silicon wafer and/or pieces of thin film as shims.
2) ALWAYS calibrate the diffractometer before starting, although this is not necessarily recommended by CCMR lab procedure. Other users FREQUENTLY leave things messed up. Calibration is CRITICAL at the small angles used for mesoporous silicates.
3) Occasionally the diffractometer may be completely locked up when one arrives at the lab to use it. Users sometimes succeed in sending the tube and/or detector to angles less than zero. If this happens, and the angles are sufficiently smaller than zero, stops on the goniometer trip microswitches disabling the axis motors. To correct this, switch the axis power to "off", and manually move the axes to positions greater than zero using the stepper knobs. Then turn axis power to "on" and BE SURE to CALIBRATE, according to standard procedure.

APPENDIX B: Pole Figure X-ray Diffraction of Mesoporous Silica Films (Procedural Notes)

These notes concern x-ray diffraction of large d-spacing (> 15 Å) films on substrates. They apply to pole figures done in reflection geometry on the "Scintag II" diffractometer in the CCMR X-ray Diffraction Facility managed by M. Weathers. As discussed in the text of this thesis, this diffractometer could not be aligned with sufficient precision to obtain accurate reflection-geometry pole figures with the incident beam at small angles. Nevertheless, the various alignment schemes that were employed are discussed below. Familiarity with these issues may simplify the process of obtaining useful pole figure data from the new diffractometer(s) being purchased from Bruker.

There are four main issues to be dealt with in this Appendix:

I. Alignment of the sample surface normal to the phi axis of the diffractometer:

II. Placement of the sample front surface at the intersection of the phi and chi axes.

III. Alignment of the collimator such that the beam hits the intersection of the phi and chi axes.

IV. Experimental development of defocus corrections.

Each of these issues will now be dealt with in turn.

I. Alignment of the sample surface normal to the phi axis of the diffractometer

1) Sample front surface alignment using rocking curves on the silicon peaks from the substrate. This method is similar to that described in 2) below, but has the possibility of being much more precise (due to limitations discussed below in the precision of the Laue method). Rocking curves were done at different values of phi, and the holder's tilt axes were adjusted in an attempt to eliminate azimuthal dependence of the results. This was very time-consuming and tedious. Also, to be effective, it would be necessary to have low-to-no miscut in the substrate, and a flat film, conditions that we did not have.

2) Sample front surface alignment using real-time back-reflection Laue camera. In this method, the sample is first mounted to the diffractometer's adjustable holder. This holder is then mounted in the Laue camera. Attempts were made to align samples mounted on the adjustable holder by using the real-time Laue camera to ensure that the (100) planes in the substrate were within +/- 0.1° of normal to what would become the phi axis once the holder is moved to the diffractometer. However, initial substrates had miscuts of as much as 1°, causing the substrate surface to be insufficiently parallel to the (100) planes for this technique to be helpful. Later efforts with substrates from Virginia Semiconductor possessing miscuts of only +/- 0.1° suggested that the Laue camera was not really accurate to +/- 0.1° as claimed, and so this method was abandoned. An

additional problem was presented by the fact that the mesoporous silica film surfaces themselves were neither smooth nor flat.

3) Sample front surface alignment using a laser. Attempts were made to align samples mounted on the adjustable holder by using a red laser reflected from the sample front surface to a white paper target some distance away. In this method, the sample holder was mounted in the diffractometer. The sample was rotated about the phi axis while observing the laser's reflection on the target. The idea was to adjust the sample holder axes so that the spot reflected on the target was motionless. Two problems were encountered with this method:

   a) The film surface was very rough. Consequently the reflection was highly non-specular and so the beam reaching the target was low in intensity and somewhat spread out spatially. Low reflected intensity necessitated a darkened room, increasing the chances for damaging one's eyes through dilated pupils via accidental intense reflections from the metal diffractometer. The spread-out beam contributed to the issue mentioned in b) below.

   b) The small x-ray scattering angle (~1.1°) necessitated exceptionally good alignment, so that it was necessary to place the target at least 2 meters from the sample to obtain sufficient resolution in the motion of the reflected light. However, at this large distance it became difficult to observe this motion while adjusting the sample holder axes.

This method was also tried after scraping the mesoporous silica film off of a small region of the substrate in order to solve issue a) above. Even with this

modification, only very poor alignment was obtained, so that this method was abandoned.

This method might be more successful if a mirror were inserted between the sample and the paper target, so that the target could be placed close to the diffractometer.

4) Sample front surface ("non-")alignment - the most successful method. The best reflection pole figure results were obtained by simply zeroing out the tilt axes on the adjustable holder as precisely as possible while viewing the axes' calibration marks under an optical microscope. This method ignored completely any real or potential lack of flatness in the substrate, film, or both. This method produced results that appeared much more reasonable than any of the three methods described above.

II. Placement of the sample front surface at the intersection of the phi and chi axes

The diffractometer has two different sample holders, an oscillating holder and an adjustable holder. Whichever holder is used, the sample surface must be placed at the intersection of the chi and phi axes. If it is not, as the holder is rotated about the chi axis, the sample will move out of the beam, or will move so as to block the beam completely. This would not happen at higher incident beam angles, but at ~1.1°, this adjustment is critical. My results suggest that I had this problem repeatedly, and I was able to confirm this with fluorescent screens.

The different holders present different problems.

The adjustable holder has a z-axis that can (in principle) be adjusted to get the surface in the desired position. In practice, this is essentially impossible, for at least 2 reasons:

1) The adjustment is continuous (as opposed to occurring in discrete steps), and is VERY coarse. There can also be significant mechanical backlash in the adjusting mechanism.

2) The method of determining the accuracy of the adjustment is very imprecise, involving as it does adjusting the sample until it blocks "about half" the incident beam intensity when the beam is at lower power and sent straight into the detector (theta = 2-theta = 0°). Since the sample is not perfectly flat, the surface is ill-defined, and it may be tilted, etc, even if one REALLY got $I/I_0 = 1/2$, once the beam was at 1.1° instead of 0°, the adjustment would be off.

The oscillating holder has different problems. In principle, it is machined so that the sample surface will be correctly positioned. In practice, I do not believe it was made with sufficient precision for our very small incident beam angles. In any case, it has too much (again, for the small angles involved) mechanical play in it. This was verified by rocking scans done on Si (100) substrates, which were found to have a significant azimuthal dependence attributable to the holder moving and not the single crystal sample.

III. Alignment of the collimator such that the beam hits the intersection of the phi and chi axes

If the collimator is positioned incorrectly on the bracket that holds it in front of the tube, similar problems as described in II above will result. That is, as the holder is rotated about the chi axis, the sample will move out of the beam, or will move so as to block the beam completely. This would not happen at higher incident beam angles, but at ~1.1°, this adjustment is critical. My results suggest that I had this problem or the related problem above repeatedly.

There are at least 2 difficulties:

1) There is really no "adjustment" for the collimator position. It must be loosened up and moved around randomly, with each position checked by trial and error. It moves too much too easily during this process. Therefore, if one has it "close" on one try, one may inadvertently end up miles away on the next. Of course, this difficulty can be minimized by taking extreme care.
2) There is no good way to tell when it is correctly aligned. Checking the zero-position of the detector works well for position in the plane in which the detector moves. This is done by setting theta = 0°, and scanning the detector across the 2-theta = 0° position at low power with a 0.1° slit to see if the peak is really at zero. However, a method must be found to check the correct position in the plane perpendicular to this. The collimator may still be too "high" or too "low".

IV. Experimental development of defocus corrections

This was not even addressed in my research, since to generate useful defocus files one must first be able to align the diffractometer properly. Assuming this happy circumstance, defocus files should be generated from test samples that are as similar to the true samples of interest as possible, except that the mesoporous silica pore orientation of the test samples MUST BE COMPLETELY RANDOM!

The defocus files used in the research reported in this thesis were created from data taken by N. Donnelly. The data was taken using uncalcined MCM-41 bulk powder from a basic synthesis (sample A05.b5n), which had a very good x-ray diffraction spectrum. The powder was ground up using a mortar and pestle, and affixed to the pole figure sample holder with tape. Theta-two theta scans were then run on the pole figure diffractometer with values of chi ranging from 270° to 360°, in steps of 5°, corresponding to 0° to 90° of tilt respectively. The intensities of the (100) peaks for chi greater than 270° were compared to the (100) peak intensity for chi = 270° in order to generate a defocus correction file.

It was found that the (100) intensities for tilts of about 5° to 20° actually exceeded the intensity for zero tilt. I believe that this was due to one or more of the alignment issues already discussed elsewhere in this thesis.

APPENDIX C: Temperature-Dependent X-ray Diffraction of Mesoporous Silica Films (Procedural Notes)

These notes concern x-ray diffraction of large d-spacing (> 15Å) films, either free-standing or on substrates. They apply to elevated temperature theta-two theta diffraction done on the "Scintag I" diffractometer in the CCMR X-ray Diffraction Facility managed by M. Weathers. Where these notes are concerned with the software that controls the diffractometer, they apply to the old VAX software. The new DMSNT Windows NT-based software from Scintag had problems interfacing with the temperature controller at the time that the author's experiments were done.

1) Elevated temperature experiments must be scheduled in advance with M. Weathers. A special hot stage must be mounted to the diffractometer, and the diffractometer must be recalibrated.
2) Just prior to mounting the hot stage on the diffractometer, a regular theta-two theta scan of the sample should be taken. This is needed to compare to preliminary scans taken on the hot stage in order to verify that the hot stage is aligned correctly.
3) After the hot stage is mounted, the sample should be scanned at room temperature and the (100) peak position and shape compared to the results obtained in step 2) above. A drop in intensity (counts) is expected, because the beam passes through two beryllium windows in the hot stage enclosure. However, the hot stage should be (re-)positioned such that the (100) peak position is the same as that found in step 2) above.

4) Temperature ramp rates can be programmed to coincide with typical rates used in calcination of samples.

APPENDIX D: Substrate Patterning and Trench Sidewall Coating by Bosch Etching

Bosch etching was explored as an alternative to depositing fluoropolymer monolayers by vapor priming substrates, and subsequently removing the monolayer from horizontal surfaces by ion milling. Bosch etching can leave a fluoropolymer monolayer as a usually unwanted side effect. By correctly programming the machine, it is possible to leave this monolayer on vertical surfaces only. Therefore this process had the possibility to meet our patterning and coating needs in essentially one step.

Experiments were performed by L. Lam, but unfortunately, all deposited fluoropolymers were inadvertently removed by a final ashing process in O_2 plasma. As a result, we were unable to test these substrates in mesoporous silica film growth experiments. However, it was learned from J. Williams of the CNF that the Bosch etcher, as part of its iterative process, leaves VERTICAL undulations in the walls of vertical features. That is, the undulations are vertical, meaning that the resulting troughs and hills in the sidewalls run horizontally. Such troughs would, according to the mesopore alignment theory being pursued, result in mesopores aligning parallel to the substrate surface rather than normal to it. Consequently, this method, even if the Bosch etching is done correctly, is unlikely to lead to vertical mesopores.

REFERENCES

1] R.P. Feynman, Int. J. Theor. Phys. **21**, 467 (1982)

2] R.P. Feynman, *Feynman Lectures on Computation*, edited by Hey and Allen (Addison Wesley, Reading, MA, 1996) ch 6

3] P.W. Shor, in *Proceedings of the 35th Annual Symposium on Foundations of Computer Science, Santa Fe, NM, 1994*, edited by Shafi Goldwasser (IEEE Computer Society Press, Los Alamitos, CA, 1994) pp124-134

4] L.K. Grover, Phys. Rev. Lett. **79**, 325 (1997)

5] C. Monroe, D.M. Meekhof, B.E. King, W.M. Itano, and D.J. Wineland, Phys. Rev. Lett. **75**, 4714 (1995)

6] I.L. Chuang, N. Gershenfeld, and M. Kubinec, Phys. Rev. Lett. **80**, 3408 (1998)

7] J.A. Jones, M. Mosca, and R.H. Hansen, Nature **393**, 344 (1998)

8] Y. Nakamura, Yu. A. Pashkin, and J.S. Tsai, Nature **398**, 786 (1999)

9] "MCM-41" is the designation given this material by Mobil Chemical Corp., in their papers announcing its discovery (cf references 10 and 11). No explanation of the acronym was given. To the author's knowledge, the meaning of this acronym has never been published.

10] C.T. Kresge, M.E. Leonowicz, W.J. Roth, J.C. Vartuli, and J.S. Beck, Nature **359**, 710 (1992)

11] J.S. Beck, J.C. Vartuli, W.J. Roth, M.E. Leonowicz, C.T. Kresge, K.D. Schmitt, C. T-W. Chu, D.H. Olson, E.W. Sheppard, S.B. McCullen, J.B. Higgins, and J.L. Schlenker, J. Am. Chem. Soc. **114**, 10834 (1992)

12] J.C. Vartuli, K.D. Schmitt, C.T. Kresge, W.J. Roth, M.E. Leonowicz, S.B. McCullen, S.D. Hellring, J.S. Beck, J.L. Schlenker, D.H. Olson, and E.W. Sheppard, Chem. Mater. **6**, 2317 (1994)

13] J.S. Beck, J.C. Vartuli, G.J. Kennedy, C.T. Kresge, W.J. Roth, and S.E. Schramm, Chem. Mater. **6**, 1816 (1994)

14] C-Y. Chen, H-X. Li, and M.E. Davis, Microporous Mater. **2**, 17 (1993)

15] C-Y. Chen, S.L. Burkett, H-X. Li, and M.E. Davis, Microporous Mater. **2**, 27 (1993)

16] A. Monnier, F. Schueth, Q. Huo, D. Kumar, D. Margolese, R.S. Maxwell, G.D. Stucky, M. Krishnamurty, P. Petroff, A. Firouzi, M. Janicke, and B.F. Chmelka, Science **261**, 1299 (1993)

17] Q. Huo, D. I. Margolese, G.D. Stucky, Chem. Mater. **8**, 1147 (1996)

18] A. Corma, Q. Kan, M.T. Navarro, J. Perez-Pariente, and F. Rey, Chem. Mater. **9**, 2123 (1997)

19] S.S. Kim, W. Zhang, T.J. Pinnavaia, Science **282**, 1302 (1998)

20] A. Karlsson, R. Schmidt, and M. Stoecker, unpublished work

21] S.A. Bagshaw, E. Prouzet, and T.J. Pinnavaia, Science **269**, 1242 (1995)

22] E. Prouzet and T.J. Pinnavaia, Angew. Chem. Int. Ed Engl. **36**, 516 (1997)

23] S.H. Tolbert, T.E. Schaeffer, J. Feng, P.K. Hansma, and G.D. Stucky, Chem. Mater. **9**, 1962 (1997)

24] M. Ogawa, Chem. Commun., 1149 (1996)

25] Q. Huo, D.I. Margolese, U. Ciesla, P. Feng, T.E. Gier, P. Sieger, R. Leon, P.M. Petroff, F. Schueth, and G.D. Stucky, Nature **368**, 317 (1994)

26] M.T. Anderson, J.E. Martin, J.G. Odinek, and P.P. Newcomer, Chem. Mater. **10**, 1490 (1998)

27] M. Antonietti, B. Berton, C. Goeltner, and H-P. Hentze, Adv. Mater. **10**, 154 (1998)

28] D. Zhao, J. Feng, Q. Huo, N. Melosh, G.H. Fredrickson, B.F. Chmelka, and G.D. Stucky, Science **279**, 548 (1998)

29] M.E. Davis, C-Y. Chen, S.L. Burkett, and R.F. Lobo, presented at the 1994 MRS Spring Meeting on April 7, 1994

30] C.J. Brinker, G.W. Scherer, *Sol-Gel Science – The Physics and Chemistry of Sol-Gel Processing* (Academic Press, San Diego, 1990) ch 1,3

31] M. Ogawa, J. Am. Chem. Soc. **116**, 7941 (1994)

32] K.R. Kloetstra, H.W. Zandbergen, J.C. Jansen, H. van Bekkum, Microporous Mater. **6**, 287 (1996)

33] H. Yang, A. Kuperman, N. Coombs, S. Mamiche-Afara, and G.A. Ozin Nature **379**, 703 (1996)

34] S. Schacht, Q. Huo, I.G. Voigt-Martin, G.D. Stucky, and F. Schueth, Science **273**, 768 (1996)

35] I.A. Aksay, M. Trau, S. Manne, I. Honma, N. Yao, L. Zhou, P. Fenter, P.M. Eisenberger, and S.M. Gruner, Science 273, 892 (1996)

36] H. Yang, N. Coombs, I. Sokolov, and G.A. Ozin, J. Mater. Chem. **7**, 1285 (1997)

37] H. Yang, N. Coombs, O. Dag, I. Sokolov, and G.A. Ozin, J. Mater. Chem. **7**, 1755 (1997)

38] J.E. Martin, M.T. Anderson, J. Odinek, and P. Newcomer, Langmuir **13**, 4133 (1997)

39] Y. Lu, R. Ganguli, C. Drewien, M.T. Anderson, C.J. Brinker, W. Gong, Y. Guo, H. Soyez, B. Dunn, M. Huang, J.I. Zink, Nature **389**, 364 (1997)

40] H. Yang, N. Coombs, and G.A. Ozin, J. Mater. Chem. **8**, 1205 (1998)

41] M.E. Gimon-Kinsel and K.J. Balkus, Jr., *Mesoporous Molecular Sieves 1998 – Studies in Surface Science and Catalysis* **117**, edited by L. Bonneviot, F. Beland, C. Danumah, S. Giasson, and S. Kaliaguine (Elsevier Science B.V. 1998) pp 111-118

42] T.W. Dalrymple, *Thesis-Master of Engineering* (Cornell University 1998)

43] Y. Takamura, *Thesis-Senior* (Cornell University 1998)

44] N. Donnelly, *Research Experience for Undergraduates Final Report* (Cornell University 1998)

45] K.J. Edler, J. Dougherty, R. Durand, L. Iton, G. Kirton, G. Lockhart, Z. Wang, R. Withers, and J.W. White, Colloids Surfaces A: Physicochem. Eng. Aspects **102**, 213 (1995)

46] K.J. Edler and J.W. White, Chem. Mater. **9**, 1226 (1997)

47] M. Trau, N. Yao, E. Kim, Y. Xia, G.M.Whitesides, and I.A. Aksay, Nature **390**, 674 (1997)

48] Y.S. Tang, G.L. Jin, K.L. Wang, H.M. Soyez, and B.S. Dunn, Proceedings of the 1997 Banff Conference on Si MBE (Molecular Beam Epitaxy)

49] Y.S. Tang, S. Cai, G. Jin, J. Duan, K.L. Wang, H.M. Soyez, and B.S. Dunn, Appl. Phys. Lett. **71**, 2448 (1997)

50] J. Liu, X. Feng, G.E. Fryxell, L-Q. Wang, A.Y. Kim, and M. Gong, Adv. Mater. **10**, 161 (1998)

51] M.J. MacLachlan, P. Aroca, N. Coombs, I. Manners, and G.A. Ozin, Adv. Mater. **10**, 144 (1998)